AECL-9383

ATOMIC ENERGY OF CANADA LIMITED

L'ÉNERGIE ATOMIQUE DU CANADA LIMITÉE

ZIRCONIUM INTERMETALLICS AND HYDROGEN UPTAKE DURING CORROSION

Alliages intermétalliques de zirconium et absorption d'hydrogène lors de la corrosion

B. COX

Chalk River Nuclear Laboratories

Laboratoires nucléaires de Chalk River

Chalk River, Ontario

April 1987 avril

ATOMIC ENERGY OF CANADA LIMITED

ZIRCONIUM INTERMETALLICS AND HYDROGEN UPTAKE DURING CORROSION

by

B. Cox

Reactor Materials Division
Chalk River Nuclear Laboratories
Chalk River, Ontario KOJ 1JO
1987 April

AECL-9383

L'ÉNERGIE ATOMIQUE DU CANADA, LIMITÉE

ALLIAGES INTERMÉTALLIQUES DE ZIRCONIUM ET ABSORPTION D'HYDROGÈNE LORS DE LA CORROSION

par

B. Cox

RÉSUMÉ

On examine les voies par lesquelles l'hydrogène peut pénétrer dans les alliages de zirconium à particules de deuxième phase lors de la corrosion. On considère à la fois la diffusion directe à travers la masse de la pellicule d'oxyde et migration à travers les particules de deuxième phase qui intersectent la surface. La vérification des résultats obtenus dans le cas de l'absorption d'hydrogène par les alliages de zirconium au cours des premières phases d'oxydation, lorsque la pellicule d'oxyde est encore cohérente, laisse supposer que, pour le Zr, le Zr-1%Cu et le Zr-1%Fe, l'hydrogène pénétre par diffusion à travers la masse de la pellicule de ZrO^2 tandis que, pour les Zircaloys, sa voie de migration principale pourrait être par les alliages intermétalliques. On examine les phases de ce dernier processus et on classe les indications obtenues sur les propriétés des alliages intermétalliques. La comparaison de ces renseignements avec les résultats obtenus dans le cas de l'absorption d'hydrogène par deux séries d'alliages ternaires (Zr-1%Nb - 1%X, Zr-1%Cu - 1%X) laisse supposer qu'une absorption d'hydrogène élevée est souvent liée à des alliages intermétalliques à hydrogène hautement soluble et vice versa. On examine les propriétés des alliages intermétalliques de $Zr(Fe/Cr)^2_{+X}$ pour tenter de comprendre le comportement des Zircaloys et on en conclu que les renseignements actuels établissant la composition et les dimensions de cellules élémentaires de ces particules intermétalliques ne sont pas assez précis pour permettre la mise en corrélation.

Division des Matériaux des réacteurs
Laboratoires Nucléaires de Chalk River
Chalk River, Ontario K0J 1J0
1987 avril

AECL-9383

ATOMIC ENERGY OF CANADA LIMITED

ZIRCONIUM INTERMETALLICS AND HYDROGEN UPTAKE DURING CORROSION

by

B. Cox

ABSTRACT

The routes by which hydrogen can enter zirconium alloys containing second phase particles during corrosion are discussed. Both direct diffusion through the bulk of the oxide film, and migration through second phase particles that intersect the surface are considered. An examination of results for hydrogen uptake by zirconium alloys during the early stages of oxidation, when the oxide film is still coherent, suggests that for Zr, Zr-1%Cu and Zr-1%Fe the hydrogen enters by diffusing through the bulk ZrO_2 film, whereas for the Zircaloys the primary migration route may be through the intermetallics. The steps in the latter process are discussed and the evidence available on the properties of the intermetallics collated. A comparison of these data with results for hydrogen uptake by two series of ternary alloys (Zr-1%Nb - 1%X, Zr-1%Cu - 1%X) suggests that high hydrogen uptakes often correlate with intermetallics with high hydrogen solubilities and vice versa. The properties of $Zr(Fe/Cr)_{2+x}$ intermetallics are examined in an attempt to understand the behaviour of the Zircaloys, and it is concluded that present data establishing composition and unit cell dimensions for such intermetallic particles are not of sufficient accuracy to permit a correlation.

Reactor Materials Division
Chalk River Nuclear Laboratories
Chalk River, Ontario K0J 1J0
1987 April

AECL-9383

1. INTRODUCTION

Many of the common impurities in zirconium, and some alloying additions added in commercial alloys, are relatively insoluble, and appear, therefore, as "precipitated particles" of intermetallic compounds. From the early days of zirconium alloy studies these intermetallic particles have been accused either of causing oxide breakdown during oxidation, or of preventing it if size and distribution were correct (1,2), and of affecting the amount of hydrogen absorbed during the corrosion process (3,4). The precise nature of the intermetallic's involvement in the corrosion process, especially in-reactor, is still argued extensively. However, recent studies (5,6) have tended to confirm that particle size and distribution must be just right (neither too large nor too small) if severe corrosion is to be avoided under all water chemistry conditions in reactor (Figure 1).

The effect of the intermetallics on hydrogen uptake was considered (3,4) to be a result of specific chemical properties of the alloying addition because of the apparently clear trend seen in the early tests (Figure 2) with position in the Periodic Table. This may correlate with the number of unpaired 3d electrons in the added element. This would vary with the effective valence of the addition, but should peak between Mn and Co. A recent reassessment of the role of chemistry in hydrogen uptake, using some previously unpublished early data (7), showed that the effect in binary zirconium alloys, or ternary alloys of the form Zr-Sn-X, was not as simple as the early results (heavily weighted by data obtained at high oxidation temperatures) suggested. However, a trend towards peak hydrogen uptakes with group VIII metals added was still evident. The results of adding similar elements to Zr-1%Nb (Figure 3a) or Zr-1%Cu (Figure 3b) binary alloys, was more complex and did not exhibit a simple trend along the series.

Renewed interest in this subject arose from observations that hydrogen uptake in Zr-2.5 wt%Nb alloy pressure tubes might be affected by the concentration of insoluble impurities in the alloy; of which iron was the major suspect. However, our knowledge of the properties and behaviour of intermetallic particles, relevant to the hydrogen uptake problem, has advanced little in the past twenty years. In general, however, it is still held that the intermetallic, or its oxidation products, can provide a site at which hydrogen atoms can gain access to the metal (4). The precise properties, and rate processes, that might be important in this context have not yet been measured. In the absence of any significant number of intermetallic sites for hydrogen entry the ingress of hydrogen may be controlled by diffusion through any ZrO_2 barrier layer on the specimen surface. Permeability of hydrogen through a ZrO_2 film is not well known (4), but is thought to be $\leq 10^{-18} cm^{-1}.s^{-1}$ at ~300°C. Thus, in the presence of a thick oxide film and the absence of intermetallics, diffusion into the metal will be controlled almost entirely by the frequency of localised flaws (cracks, pores, impurity segregation) in the oxide film. The big difference in the normal hydrogen uptake rate between Zircaloy-2 and Zr-2.5 wt%Nb is thought to result from the presence of a much thicker barrier layer oxide, and the infrequency of intermetallics, for the latter (8-10).

It may, therefore, be important to measure some of the relevant physical properties of zirconium intermetallics, if these differences are to be understood, and present commercial alloys improved. As a start to this understanding the properties that might be important in the hydrogen uptake mechanism are discussed in this report, and the knowledge available in the literature is reviewed. Since much of this is derived from work related to hydrogen storage, there are major gaps in the information. While absorption and desorption, stability of hydrides, and factors controlling the amount of hydrogen absorbed, have all been studied extensively, properties such as hydrogen diffusion rates in intermetallics, that are important to understanding corrosion problems, have received essentially no attention.

2. THE HYDROGEN UPTAKE PROCESS

For hydrogen atoms entering zirconium by way of an intermetallic particle, as opposed to those entering by diffusion through the residual barrier layer of oxide at the metal/oxide interface, the following steps are perceived as being important:

(i) Discharge of a proton on the surface of whatever oxide covers the intermetallic by an electron emerging from the zirconium metal. In some special cases (e.g. Zr/Ni intermetallics) direct dissociation of molecular hydrogen can occur.

(ii) Competition between the hydrogen atom recombination reaction and the permeation of hydrogen atoms through whatever oxide film covers the intermetallic.

(iii) Transport of hydrogen across the intermetallic. The diffusivity of hydrogen in the intermetallic is comprised of the diffusion coefficient for hydrogen under the appropriate conditions of temperature and fugacity, the mean concentration of hydrogen in the intermetallic and the concentration gradient set by the interfacial conditions.

(iv) The transfer of the hydrogen from the intermetallic particle to the zirconium metal matrix.

It will be appropriate to consider each step in the process to see what evidence there is that will support the overall hydrogen uptake scenario. For hydrogen migrating through a coherent oxide film on an intermetallic-free alloy, a series of steps similar to i-iii above will occur, and this entry mechanism will also operate in parallel with entry via the intermetallics on other alloys.

3. WHAT WE KNOW

(i) Surface Reactions

Surprisingly little work has been done on the surface reactions that occur on zirconium, compared with work on other transition metals, and even less on the more relevant oxide covered zirconium surface. Sticking factors for the common gases (O_2,N_2,CO_2,CO,H_2O) on clean zirconium surfaces have been measured (11,12) and are observed to be unity initially, and then to decrease rapidly (Figure 4), although the precise point of onset of this drop may be in dispute (92). However, a more practical and typical situation of a zirconium surface with a relatively thick barrier layer oxide has not been studied, and useful reactions such as the hydrogen recombination reaction on these surfaces remain uninvestigated. Because of the extensive use of ZrO_2 as a catalyst in the chemical industry, the reactions between gaseous species (H_2O,CO_2,CO) adsorbed on ZrO_2 surfaces have been studied (13,14). In the absence of a metal substrate, however, the cathodic component of the thermal oxidation reaction is absent in these studies. Nevertheless, they do give indications of the expected formation rates of formic acid, methanol and bicarbonate species on ZrO_2 surfaces that may be useful in interpreting the buildup of various species in CO_2-filled reactor annuli.

The rates of the surface reaction of O_2 and H_2O on oxide covered zirconium alloys may limit the initial rate of oxide thickening when a specimen preheated in vacuum has reactive species admitted to it. If cubic (or parabolic) oxidation kinetics were followed by zirconium alloys from the start, they should extrapolate back to an infinite rate at zero time. In practice a short, almost linear period of oxidation is observed at the start of vacuum microbalance experiments. These rates have been measured at 400-600°C (15) and, although transients resulting from the mode of starting the experiment may play a major part in determining these initial rates, the observation that initial rates measured in H_2O vapour were usually much less than those measured in O_2 (even though little difference was seen in the later diffusion controlled oxidation rates) suggests a real difference in the surface reaction rates of the two species on oxide covered zirconium alloys (Figure 5). The sticking coefficients calculated from these curves lie between 10^{-7} and 10^{-8} for both O_2 and H_2O. These are in reasonable agreement with results from Figure 4, if extrapolated to an initial oxide of ~10 monolayers (~11 x 10^{15} molecules/cm^2).

No measurements are known of the comparable reaction rates of gases on zirconium intermetallic surfaces; a more useful number for assessing Zircaloy behaviour than the general reaction on a zirconium surface. Of particular importance for modelling hydrogen uptake will be results on the hydrogen recombination reactions on ZrO_2, doped ZrO_2, and other oxides such as Fe_2O_3, Fe_3O_4 on ZrO_2.

(ii) Permeability of ZrO_2 Films

Despite much early work (4) no believable measurement of the diffusion coefficient of hydrogen in ZrO_2 or of the permeability of a coherent ZrO_2 film has been published. All published work suffers from the problem of establishing whether or not the hydrogen migration occurred via physical flaws in the oxide (4). Attempts to measure lattice diffusion by NMR or nuclear reaction techniques have either not progressed significantly or have shown the techniques to be inadequate in spatial resolution or sensitivity (16,17), however, preliminary results indicate diffusion coefficients much lower than the published ones (4).

In the early stages of oxidation, where oxide films are coherent, but hydrogen concentrations are low, it is difficult to get a good measure of the hydrogen uptake kinetics. Some data have been obtained during the early stages of oxidation by using thin zirconium alloy foils (7,18,19), and the results have usually been plotted as hydrogen uptake versus oxygen uptake. The data for Zircaloy-2 in steam have been replotted individually as a function of time (Figures 6 and 7), to examine the possibility that for these alloys the hydrogen is gaining admission via the oxide over second phase particles.

A comparison of the two modes of plotting the data is very revealing (cf. Figures 6 and 7 with Figure 13). When individually plotted against time it is evident that the oxidation curves and the hydrogen uptake curves follow different kinetics, especially at low temperatures. At 300 and 350°C the growth of the thin interference colour oxide film is essentially linear up to an average thickness of ~0.2 μm when the normal, near-cubic pretransition kinetics ensue. During the linear oxidation period the hydrogen uptake kinetics are close to parabolic, becoming nearly identical with the oxidation kinetics during the second stage. This suggests that in the initial period the hydrogen uptake is diffusion controlled by a barrier that increases in thickness with time, but that this barrier is different from the one controlling the growth of the oxide film. Hydrogen migration may, therefore, be occurring by an alternative route through the oxide on the intermetallics. During the second stage both the oxidation and the hydrogen uptake appear to be controlled by the same barrier, namely diffusion through the coherent ZrO_2 film on the matrix. The breakdown of this barrier at the transition point is signalled very clearly by an increase in hydrogen uptake rate and a change to linear uptake kinetics. A comparison of the oxidation and hydrogen uptake curves shows that the transition in the hydrogen uptake curve precedes that in the oxidation curve. This was to be expected from other work that showed porosity developing in the oxide film before a major change in the oxidation kinetics was detectable (20).

The few results available on the ICI 0.005" batch of Zircaloy-2 at other pressures (0.016 and 33.3 atm.) suggest that neither the hydrogen uptake nor the oxidation curves are significantly affected by pressure over this range. When we study the oxidation and hydrogen uptake curves in air (saturated in water vapour at room temperature), however, we see significant differences (Figures 8,9) from the curves in steam. The pretransition oxidation kinetics

are slower in air than in steam, although they still show an initial linear period and a later (approximately) cubic kinetic period. The initial linear rates in air are only about one-third those in steam, and because of this the initial linear period becomes visible at 400°C in air, whereas in steam it was already past at the shortest exposure time employed. The oxidation curves in air show a regular trend with increasing temperature, whereas the hydrogen uptake curves prior to the onset of the oxidation rate transition are almost athermal at 350-500°C. The 350°C results are just separable from the scatter of the higher temperature data, and only the 300°C data are significantly below the others. The 300°C uptake curves again show a two-stage (parabolic → cubic) form with the break at the end of the initial linear oxide growth period. The hydrogen uptake kinetics again appear to be diffusion controlled. Since the rates in water vapour are the same as in atmospheric pressure steam, whereas they are lower in air with an equal water vapour partial pressure, the difference can be ascribed either to the effect of oxygen on the hydrogen recombination reaction, or to a modification of the oxide formed over the intermetallics.

In contrast to those for Zircaloy-2, the hydrogen uptake curves (ΔH vs ΔO) for van Arkel Zr, Zr-1%Cu and Zr-1%Fe alloys (20) are linear in the pretransition region (Figures 10-13). These results suggest that the hydrogen uptake kinetics (weight gains vs time not available) are the same as the oxidation kinetics, and thus, that in these alloys the hydrogen uptake rate is controlled by diffusion through the bulk of the oxide film.

The properties of the oxide films formed on intermetallics have not been investigated widely. The phases formed on Zr/Fe intermetallics during oxidation are several (ZrO_2,Fe_2O_3,Fe_3O_4,α-Fe,Zr_3FeH, etc.) suggesting a very complicated layer structure (21). This situation was confirmed by Ploc (22), who has shown further that the behaviour of Fe, Cr and Ni in binary intermetallics differs, and that the behaviour of ternaries comprising two out of these three transition metals is different again. Such differences in the behaviour of binary and ternary intermetallics could account for the differing, effects of the same alloying additions on hydrogen uptake by Zr-Nb or Zr-Cu alloys. In the first instance only binary intermetallics will be precipitated whereas in the second ternary intermetallics with Cu may result.

Although there is an extensive literature on the properties of zirconium intermetallics for use as hydrogen storage materials, in most instances these are not the same intermetallics as those occurring in the structural zirconium alloys. However, the factors that lead to variation in hydrogen uptake behaviour by the hydrogen storage materials may be the same factors that affect hydrogen uptake of the structural alloys. Some of these properties have been collected in Table 1.

From the point of view of understanding the variability in the surface barrier film on the intermetallic to hydrogen permeation, only results on the preconditioning treatments to promote rapid hydrogen uptake are relevant. Descriptions of this preconditioning were often omitted, or only referred to cursorily, when the work was written up. However, it is evident that the

properties of the surface barrier film on the intermetallics vary enormously. Some intermetallics need no preconditioning before rapid hydrogen uptake is obtained whereas others require many hydrogenation cycles at elevated temperature to break down the surface barrier, and sometimes to cause fragmentation of the sample. Since details of the physical nature of the oxide on these intermetallics are universally absent, only qualitative data on the factors affecting the permeability of the surface oxide films can be gleaned. For instance, in the $ZrMn_x$ intermetallics, manganese has been shown to be preferentially oxidised (44,62) but the nature of the layer was not investigated.

These results suggest that the ternary elements present in the intermetallic are critical to the formation of permeable surface oxide barriers; the binary intermetallics are generally much more difficult to hydride even with preconditioning. Additionally, the presence of hyperstoichiometry in the intermetallic seems to induce permeability in the surface oxide barrier. Nevertheless, little useful evidence on the permeability of surface films is available from the studies of hydrogen storage alloys.

(iii) Diffusion Through Intermetallics

For hydrogen ingress in the early stages of oxidation via the intermetallics, (in parallel with diffusion through the intervening oxide film) once the hydrogen has entered the intermetallic (through the surface films formed on it) it must traverse the remaining unoxidised intermetallic before reaching the Zr/intermetallic boundary. At greater oxide thickness the intermetallic may get cut off from the metal by preferential oxidation along the intermetallic/matrix boundary. By this time, however, the oxide film is probably highly porous. The rate of hydrogen migration through the intermetallic is the product of three factors; the diffusion coefficient in the intermetallic; the concentration gradient across it; and the mean concentration in the intermetallic.

Essentially no information on the first of these quantities is available from studies of potential hydrogen storage alloys, because these have often been conducted on powdered intermetallics where the surface film is the most important barrier. There is little evidence from which the hydrogen fugacity at either the surface film/intermetallic or the intermetallic/α-zirconium interfaces could be estimated, so that the concentration gradient across the intermetallic remains an unknown. There is, however, a wealth of evidence on the maximum hydrogen solubility in zirconium intermetallics (Table 1).

Although much of the evidence summarised in Table 1 is on intermetallics that are of no relevance to interpreting hydrogen uptake rates in commercial zirconium alloys, the effect of a number of variables on hydrogen solubility in these intermetallics may nevertheless offer some clues as to the topics that should be investigated when studying intermetallics in zirconium structural alloys. Some of the important factors can be summarised as follows:

a) Among the ZrM_2 intermetallics there is a wide range of solubilities for hydrogen. These solubilities range (in increasing order) from $ZrFe_2$ and $ZrCo_2$ (very low and disproportionate) through $ZrAl_2H_{0.5}$, $ZrMo_2H_{0.78}$, $ZrMn_2H_{3.8}$, $ZrCr_2H_{4.1}$ to $ZrV_2H_{5.5}$.

b) Some ZrM and Zr_2M intermetallics (e.g. $ZrCoH_{2.6}$, $ZrNiH_3$, $Zr_2PdH_{2.7}$) have high hydrogen solubilities, but most disproportionate into ZrH_2 and the next higher intermetallic.

c) Oxygen and nitrogen have high solubilities in some intermetallics and both stabilize the structure and give high hydrogen solubilities in an otherwise low solubility intermetallic (e.g. $Zr_3V_3OH_{5.5}$, $Zr_3V_3NH_X$, $Zr_4Fe_2O_{0.6}H_{5.4}$, $Zr_4Pd_2OH_{4.7}$).

d) Ternary intermetallics between ZrM_2 compounds with (respectively) low and high hydrogen solubilities can show a high solubility with a relatively small concentration of the high hydrogen solubility addition (Figure 14). Examples that have been extensively studied are the $ZrFe_{2-X}Mn_X$ and $ZrFe_{2-X}Cr_X$ systems. The stability of the hydride, as shown by the dissociation pressure, and the permeability of the surface barrier vary widely across the spectrum.

e) Some intermetallic systems (e.g. $Zr(Mn/Fe)_{2+X}$, $Zr(Fe/Cr)_{2+X}$) can show significant hyperstoichiometry. This is achieved by substitution of one of the elements on Zr lattice sites. The result is a large contraction in the unit cell parameters. In very broad terms alloy additions that expand the unit cell increase the hydrogen solubility, while additions that contract the cell reduce it through an effect on the size of the interstitial sites. The most startling example of the latter effect is the reduction in hydrogen solubility resulting from hyperstoichiometric additions of Co to ZrMnFe, while the most interesting effect of the former is the large increase in hydrogen solubility in $ZrFe_2$ resulting from small additions of Al (Figure 15).

As a diagnostic tool, therefore, the unit cell parameters of intermetallics in structural zirconium alloys should be measured accurately together with accurate analyses of the precipitates for elements (e.g. O,N,Al,Mn) that might have a profound effect on their properties, in addition to the more usual estimates of Fe, Cr and Ni contents.

(iv) Oxygen Diffusion Zone in Zr

The oxygen diffusion zone in the zirconium adjacent to the oxide film has been known to perturb the distribution of hydrogen in solution and hydride precipitates since the early autoradiographic studies of Roy (63). These studies employed high temperature oxidation treatments to develop oxygen diffusion zones deep enough to be easily resolved by the autoradiographic technique. At normal reactor operating temperatures the diffusion zone is

too thin to be resolved by this technique, and the presence of a peak in the hydrogen concentration profile similar to those observed after higher temperature oxidation (Figure 16) remained unestablished. Recent studies (64) by a nuclear reaction technique have shown that this peak is present at low temperatures. Furthermore, the hydrogen concentration in this peak was found to be much higher than that either in the oxide or the bulk metal.

This high concentration of hydrogen, apparently in solid solution, was ascribed to an interaction between oxygen and hydrogen in solution in zirconium. The hydrogen peak occurs in the dilute part of the oxygen diffusion profile at a critical oxygen concentration range of ~4000-8000 ppm. There is no direct evidence that the mobility of hydrogen in this peak is significantly reduced, or that this region represents a barrier to hydrogen diffusion into the bulk metal. However, the observation that, in specimens of different thickness produced from a single batch of Zircaloy-2, the hydrogen uptake in the thinner samples (Figure 17) is slowed in comparison to the thicker specimens once the solubility at the oxidation temperature is exceeded, could be considered to be evidence for a retarding action of this hydrogen peak.

4. CORRELATION OF HYDROGEN UPTAKE BEHAVIOUR WITH INTERMETALLIC PROPERTIES

The profiles of the initial hydrogen uptake curves for Zr, Zr-1%Cu, Zr-1%Fe and Zircaloy-2 (Figures 10-13) show that the first three are possibly controlled by hydrogen diffusion through the bulk oxide, whereas only the Zircaloy-2 shows high initial hydrogen uptake percentages thought to indicate migration through the intermetallics. It is probable that only the intermetallics in Zircaloy-2 would have a high solubility for hydrogen based on the data collected here. In this oxide thickness range investigations show virtually no pores or cracks in the oxide film.

An examination of the effect of ternary additions to Zr-1%Nb and Zr-1%Cu (Figures 3a and 3b) on the hydrogen uptake behaviour does not give an ideal correlation. In the Zr-1%Nb-1%X alloys (Figure 3a), where the intermetallics precipitated would be mainly the binaries Zr_pX_q some of the elements giving binary intermetallics with high hydrogen solubilities show high hydrogen uptakes at 300-350°C (e.g. Mn,Pd) whereas those giving intermetallics with possibly low hydrogen solubilities (e.g. Fe,Cu,Mo) result in alloys with lower hydrogen uptakes. The major exception is the vanadium alloy, whose intermetallic (if ZrV_2) would have the highest hydrogen solubility, yet the alloy has among the lowest hydrogen uptake rates. However, $ZrV_2H_{5.5}$ has the lowest hydrogen equilibrium pressure of any intermetallic that has been reported, so perhaps despite its high solubility for hydrogen the hydrogen permeability through it is low. These correlations are not maintained as the oxidation temperature is increased, perhaps because of dissociation of the intermetallic hydride at high temperatures.

For the Zr-1%Cu-1%X alloys (Figure 3b), vanadium additions that might be expected to increase the hydrogen solubility in the Zr/Cu intermetallic (if they formed a ternary intermetallic) produce only a small increase at 300°C, but do result in larger increases in hydrogen uptake at higher temperatures. Pd additions similarly result in large increases in hydrogen uptake, as might be expected from their possible effect of raising the hydrogen solubility in the intermetallic. Conversely, Mo additions that should not have such an effect have only small effects on hydrogen uptake.

When taken overall these results suggest that high hydrogen uptake rates in the alloys correlate in many instances with high hydrogen solubilities in the intermetallics, provided the dissociation pressure of the hydride is not too low. This remains equally true when Zr-Ni alloys (not studied here) and the differences between Zircaloy-2 and Zircaloy-4 are considered. Thus, if we had measurements of hydrogen permeability through these intermetallics we might find a better correlation, since the assumption made above that low dissociation pressure could imply low diffusivity in the intermetallic is not well founded.

In the absence of the necessary data, it is hardly surprising that there are prominent exceptions (e.g. V) to any attempted correlation. Other factors, such as the nature of the oxide barrier on the intermetallic, may be equally or more important in many instances. We have no evidence on the compositions of the intermetallics in most of these alloys and can pursue these hypotheses, therefore, only for Zircaloy-2 and Zircaloy-4, where extensive analyses of intermetallics have been made.

5. INTERMETALLICS IN THE ZIRCALOYS

Both Zircaloy-2 and Zircaloy-4 contain two types of intermetallic particles. In the former they are primarily $Zr(Fe/Cr)_2$ and $Zr_2(Fe/Ni)$, while in the latter the majority are $Zr(Fe/Cr)_2$ with any excess Fe (especially in high-iron batches) present as either Zr_2Fe or Zr_3Fe. Studies show that the $Zr(Fe/Cr)_2$ phase can exist with either the cubic (C15) or hexagonal (C14) structure and that the proportions of these, together with the Fe:Cr ratio in the intermetallics, can vary with heat treatment, fabrication route and with batch chemistry. Structure and composition can change during irradiation as elements preferentially diffuse out of the intermetallics (65,66).

Results for structure determinations and analyses of intermetallics in the Zircaloys are summarised in Table 2. In no instance has an analysis for impurity elements (e.g. O,N,Al,Mn) in the intermetallic, or in the zone around it, been made. In fact the physical methods for obtaining such analyses, if impurities are present in low concentrations, are probably not widely available. In a few instances stray impurities (Cu,Sn,Si) have been recorded in the precipitates. In the case of Sn and Cu some scepticism should always be applied since the Sn signals may have come from the matrix, and the Cu

signals from the microscope. Few investigators appear to have taken "hole" counts or matrix counts adjacent to precipitates, with normalisation to the ZrK_{α} peak. Most cell parameters have been determined in the electron microscope, and have been of relatively low accuracy compared with X-ray data in Table 1, even though current techniques (especially the convergent beam technique) would permit much more accurate results.

An examination of Table 2 shows that in virtually no instances have both the intermetallic cell parameters and analyses been obtained with sufficient accuracy to permit a good comparison with the $Zr(Fe/Cr)_{2+x}$ structures (Figure 18) obtained from bulk intermetallics, or for the $Zr_2(Fe/Ni)$ phase in Figure 19 (84). However, in general the cell dimensions and Fe:Cr ratios are not unreasonable when compared with each other. A more detailed analysis of the structures is not possible with the present evidence.

A more surprising observation, in view of the data on bulk intermetallics, is the common observation of $Zr(Fe/Cr)_2$ particles with both C14 and C15 structures or with "polytype" structures combining the two. Although $ZrFe_2$ occurs only in the C15 (cubic) structure, $ZrCr_2$ occurs either as C14 (hexagonal) or C15 depending on heat treatment (85,86). In bulk intermetallics, for Fe:Cr ratios <5 the normal structure is C14. Of all the investigators of these compounds only Ivey and Northwood (53) report two-phase products (C14 + C15). It seems probable that the observations of the C15 structure at room temperature indicate either stabilisation by some impurity or incomplete mixing (since the C15 cell parameters reported are close to $ZrFe_2$) but no analyses have been made to examine these points. The general lack of concurrent accurate analyses and cell dimensions renders further speculation on this point unprofitable.

The observations of the body-centred tetragonal Zr_2Fe phase in some batches of Zircaloy-4 (Table 2) are also surprising, since the consensus on the Zr-Fe phase diagram (87) concludes that this phase is only produced by decomposition of Zr_3Fe at temperatures above 885°C (a temperature not usually reached during tube fabrication). Partial stabilisation by O_2 or N_2 may be involved although full stabilisation would transform it to the cubic Ti_2Ni structure (51,88,89). Again, we need more accurate cell parameters and analyses.

Of the differences between Zircaloy-2 and Zircaloy-4 that might be used to explain the difference in hydrogen uptakes, clearly the elimination of $Zr_2(Fe/Ni)$ precipitates is the primary reason. Although there are no studies of hydrogen solubility in intermetallics of this ternary system, with an Fe:Ni ratio close to unity the intermetallic properties would be expected to be close to those of the high hydrogen solubility phase (Zr_2Ni). There is a distinct trend for Fe:Cr ratios in the $Zr(Fe/Cr)_2$ phase to be higher in Zircaloy-4 than in Zircaloy-2, as might be expected because of the replacement of Ni with Fe in the former. The intermetallic data (Table 1) show that this higher Fe:Cr ratio would lower the hydrogen solubility in the $Zr(Fe/Cr)_2$ intermetallics, so this might also contribute to the reduction in hydrogen

uptake. The observations (90,91) that hydrogen uptake by Zircaloy-4 was higher than that of Low-Ni Zircaloy-2 (Ni removed, no increase in Fe) may suggest that the C16 (Zr_2Fe/Ni) phase is the major contributor to high hydrogen uptakes. This phase seems to occur in both Zircaloy-2 and -4 (although in the latter it does not contain Ni), but would probably be absent from low Ni Zircaloy-2 because of its relatively low Fe content compared with Zircaloy-4.

At present it seems to be impossible to proceed further in analysing the effect of intermetallics on hydrogen uptake by zirconium alloys. However, this attempted analysis has pointed out the importance of measuring accurately and simultaneously both the composition and the cell parameters of the intermetallics present.

6. CONCLUSIONS

Despite the wealth of data on zirconium intermetallics as hydrogen storage alloys the specific information that would permit us to assess the permeability of the various intermetallic phases to hydrogen is absent. Attempts to estimate whether these permeabilities might be high or low based on hydrogen solubilities in the intermetallic, and the dissociation pressures of the intermetallic hydrides founder because of these critical gaps in the information.

Hence, although there seems to be a rough correlation between high hydrogen uptakes in some zirconium alloys and a combination of high hydrogen solubility and high hydrogen volatility (dissociation pressure) for the intermetallics that may be present, the correlations cannot be pursued to a definite conclusion.

Analysis of some early data on hydrogen uptake by Zircaloy-2, van Arkel zirconium, Zr-1%Cu and Zr-1%Fe alloys showed from the kinetics of uptake that the mechanism of hydrogen uptake was different in Zircaloy-2 from the others. The linear relationship between ΔH and ΔO in all except Zircaloy-2 suggested diffusion through the bulk of the oxide was the controlling process during pretransition oxidation, whereas for Zircaloy-2 an additional route through the intermetallics seems to contribute the most to hydrogen ingress. An assessment of the structure and composition of intermetallics in Zircaloy-2, Low-Ni Zircaloy-2 and Zircaloy-4 suggests that the presence or absence of C16 (Zr_2Fe/Ni) precipitates could explain the observed differences between hydrogen uptake behaviour of these alloys. Accurate simultaneous measurements of intermetallic composition and unit cell parameters, coupled with hydrogen permeability studies would be needed before progress in explaining the phenomena can be made.

REFERENCES

1. B. Cox, Prog. In Nucl. En., Ser. IV, Vol. 4, p. 166, Ed. C.M. Nicholls, Pergamon, London, 1961.

2. B. Cox, J. Electrochem. Soc., 1961, 108, 24.

3. B. Cox, M.J. Davies and A.D. Dent, U.K.A.E.A. Report, AERE-M621 (1960).

4. B. Cox, Atomic Energy of Canada Ltd., Report AECL-8702 (1985).

5. F. Garzarolli and H. Stehle, "Behaviour of Core Structural Materials in Light Water Cooled Power Reactors", Presented at Int. Symp. on Improvements in Water Reactor Fuel Technology and Utilization, Stockholm, 15-19 Sept. 1986, IAEA-SM-228/24.

6. T. Andersson, T. Thorvaldsson, A. Wilson and A.M. Wardle, "Influence of Thermal Processing and Microstructure on the Corrosion Behaviour of Zircaloy-4 Tubing", Presented at Int. Symp. on Improvements in Water Reactor Fuel Technology and Utilization, Stockholm, 15-19 Sept. 1986, IAEA-SM-288/59.

7. B. Cox, Unpublished Results at AERE Harwell (1963).

8. V.F. Urbanic, B. Cox and G.J. Field, "Long-Term Corrosion and Deuterium Uptake in CANDU-PHW Pressure Tubes", Presented at 7th Int. Conf. on Zirconium in the Nuclear Industry, Strasbourg, 24-27 June 1985, ASTM-STP-939 to be published.

9. B. Cox, J. Nucl. Mat., 1987, (to be published).

10. B. Cox, Atomic Energy of Canada Ltd., Report AECL-9382 (1987).

11. C.M. Quinn and M.W. Roberts, Trans. Far. Soc., 1963, 59, 985.

12. E. Fromm and O. Mayer, Surface Science, 1978, 74, 259.

13. N.B. Jackson and J.G. Ekerdt, J. Catal., 1986, 101, 90.

14. R.G. Silver, N.B. Jackson and J.G. Ekerdt, ACS Symposium Series, "Catalytic Activation of Carbon Dioxide", ACS, New York, 1986.

15. B. Cox, J. Electrochem. Soc., 1962, 109, 6 and U.K.A.E.A Report AERE-R4348 (1963).

16. J. Sawicki, Measurement of D_2 Profile in Oxide Film by Forward Scattering, unpublished results at CRNL.

17. A. Stern, D. Khatamian, T. Laursen, G.C. Weatherly and J.M. Perz, J. Nucl. Mat., 1987, 144, 35.

18. B. Cox, U.K.A.E.A. Report, AERE-4348 (1963).

19. B. Cox and J.A. Read, U.K.A.E.A. Report, AERE-4459 (1963).

20. D.W. Freer, D.R. Silvester and J.N. Wanklyn, Corrosion, 1965, 21, 137 and AERE Report 4531 (1964).

21. Yu. F. Babikova, P.L. Gruzin, A.V. Ivanov, V.P. Filippov, I.I. Shtan', V.A. Tchaikovski and V.N. Abramtsev, "Metallurgiya I Metallovedenie Chistykh Metallov, 1976, 12, 20; CRNL Trans. by J. Sawicki (1987).

22. R.A. Ploc, unpublished results.

23. D. Shaltiel, I. Jacob and D. Davidov, J. Less. Comm. Met., 1977, 53, 117.

24. D. Fruchart, ibid., 1980, 73, 363.

25. A. Pebler and E.A. Gulbransen, Trans. AIME, 1967, 239, 1593.

26. H. Oesterreicher, Mat. Res. Bull., 1978, 13, 83.

27. R.M. van Essen, J. Less. Comm. Met., 1979, 64, 277.

28. G.G. Libowitz, H.F. Hayes and T.R.P. Gibb, Inorg. Chem., 1957, 62, 76.

29. D. Shaltiel, J. Less. Comm. Met., 1980, 73, 329.

30. I. Jacob and D. Shaltiel, Sol. State Comm., 1978, 27, 175.

31. C. Boffito, F. Doni and L. Rosai, J. Less. Comm. Met., 1984, 104, 149.

32. J.J. Didisheim, K. Yvon, D. Shaltiel, P. Fischer, P. Bujard and E. Walker, Sol. State Comm., 1979, 32, 1087 and J. Less Comm. Met., 1980, 73, 355.

33. M.H. Mendelsohn and D.M. Gruen, Proc. Int. Symp. on Metal/Hydrogen Systems, Miami Beach, 1981, p. 691, Pergamon, NY.

34. A. Pebler and E.A. Gulbransen, Electrochem. Tech., 1966, 4, 211.

35. T. Jacob, A. Stern, A. Moran, D. Shaltiel and D. Davidov, J. Less Comm. Met., 1980, 73, 369.

36. D. Fruchart, A. Roualt, C.B. Shoemaker and D.P. Shoemaker, ibid., 1980, 73, 363.

37. V.K. Sinha, G.Y. Yu and W.E. Wallace, ibid., 1985, 106, 67.

38. H. Fujii, V.K. Sinha, F. Pourarian and W.E. Wallace, ibid., 1982, 85, 43.

39. G.Y. Yu and W.E. Wallace, J. Sol. State Chem., 1986, 65, 356.

40. R.M. van Essen and K.H.J. Buschow, Mat. Res. Bull., 1980, 15, 1149.

41. J.J. Didisheim, K. Yvon, D. Shaltiel and P. Fischer, Sol. State Comm., 1979, 31, 47.

42. Y. Komazaki, M. Uchida, S. Suda, A. Suzuki, S. Ono and N. Nishimiya, J. Less. Comm. Met., 1983, 89, 269.

43. A. Suzuki, N. Nishimiya and S. Ono, ibid., 1983, 89, 263.

44. F. Pourarian, H. Fujii, W.E. Wallace, V.K. Sinha and H.K. Smith, J. Phys. Chem., 1981, 85, 3105.

45. F. Pourarian and W.E. Wallace, J. Less. Comm. Met., 1985, 107, 69.

46. D.G. Ivey and D.O. Northwood, Int. J. Hydr. En., 1986, 11, 583.

47. M.H. Mendelsohn and D.M. Gruen, J. Less. Comm. Met., 1980, 74, 449.

48. V.K. Sinha, F. Pourarian and W.E. Wallace, ibid., 1982, 87, 283.

49. G.Y. Yu, F. Pourarian and W.E. Wallace, ibid., 1985, 106, 79.

50. S.M. Fries, F. Aubertin, H.G. Wagner and U. Gonser, Z. Phys. Chemie N.F., 1985, 145, 155.

51. F. Aubertin, U. Gonser and S.J. Campbell, J. Phys F:Met Phys., 1984, 14, 2213.

52. F. Aubertin, U. Gonser and S.J. Campbell, J. Less. Comm. Met., 1984, 101, 437.

53. D.G. Ivey and D.O. Northwood, J. Mat. for En. Syst., 1983, 4, 222.

54. S.J.C. Irvine and I.R. Harris, Proc. of Conf. on "?,p 431.

55. A.V. Iridova, V.A. Somenkov, S.Sh. Shil'shstein, L.N. Padurets and A.A. Chertkov, Kristallografiya, 1978, 23, 1044 (Tr. Sov. Phys. Cryst., 1978, 23, 591).

56. W.L. Korst, J. Phys. Chem., 1962, 66, 370.

57. D.G. Westlake, H. Shaked, P.R. Mason, B.R. McCart and M.H. Mueller, J. Less. Comm. Met., 1982, 88, 17.

58. A.J. Maeland, ibid., 1983, 89, 173.

59. R. Kadel and A. Weiss, ibid., 1979, 65, 89.

60. A.J. Maeland and G.G. Libowitz, ibid., 1980, 74, 295.

61. M.H. Mendelsohn, Proc. 4th World Hydrogen Energy Conf., June 13-17, 1982, Pasadena, Ca; Eds Veziroglu, van Vorst and Kelley, Pergamon, Oxford, 1982.

62. L. Schlapbach, J. Less. Comm. Met., 1983, 89, 37.

63. C. Roy, Atomic Energy of Canada Ltd., Report AECL-2085 (1964).

64. G.C. Weatherly and A. Stern, to be published.

65. M. Griffiths, R.W. Gilbert and B.A. Cheadle, Atomic Energy of Canada Ltd., Report AECL-8852 (1985).

66. W.J.S. Wang, R.P. Tucker, B. Cheng and R.B. Adamson, J. Nucl. Mat., 1986, 138, 185.

67. G. Ostberg, ibid., 1962, 7, 103.

68. E. Vitikainen and P. Nenonen, ibid., 1978, 78, 362.

69. P. Chemelle, D.B. Knorr, J.B. van der Sande and R.M. Pelloux, ibid., 1983, 113, 58.

70. J.B. van der Sande and A.L. Bement, ibid., 1974, 52, 115.

71. J.M. Grange, D. Charquet and L. Moulin, Proc. V Int. Conf. on Zr in the Nuclear Industry, Boston, 1980, ASTM-STP-754, p. 96.

72. R.A. Versaci and M. Ipohorski, ibid., 1979, 80, 180.

73. V. Krasevec, ibid., 1981, 98, 235.

74. A. Miquet, D. Charquet and C.H. Allibert, ibid., 1982, 105, 132.

75. N.V. Bangaru, ibid., 1985, 131, 280.

76. Xian Ying Meng and D.O. Northwood, J. Less. Comm. Met., 1986, 125, 33.

77. P. Rudling, K. Lundblad Vannesjö, G. Vesterlund and A.R. Massih, Proc. VII Int. Conf. on Zr in the Nuclear Industry, Strasbourg, June 24-27, 1985, ASTM-STP-939, (to be published).

78. R.J. Comstock, J. Greggi and G.P. Sabol, ibid., (to be published).

79. N.V. Bangaru, R.A. Busch and J.H. Schemel, ibid., (to be published).

80 R. Kohli, A. Skidmore, C.T. Wang and C. Eucken, Proc. of KTG Workshop on "Second Phase Particles in Zircaloys", Erlangen, July 1-2, 1985, (to be published).

81. W.J.S. Yeng, R.P. Tucker, B. Cheng and R.B. Adamson, ibid (to be published).

82. R. Kuwae, J. Kawashima, K. Sato and E. Higashinakagawa, ibid., (to be published).

83. R. Kuwae, K. Soto, E. Higashinakagawa, and S. Nakamura, ibid., (to be published).

84. E.E. Havinga, H. Damsma and P. Hokkeling, J. Less. Comm. Met., 1972, 27, 169.

85. W. Rostoker, Trans. AIME, 1953, 197, 304.

86. Yuan-Shon Shen and O.G. Paasche, ibid., 1968, 242, 2241.

87. F. Aubertin, U. Gonser, S.J. Campbell and H.G. Wagner, Z. Metall., 1985 76, 237.

88. M.V. Nevitt, J.W. Downey and R.A. Morris, Trans. AIME, 1960, 218, 1019.

89. Yu B. Kuz'ma, V. Ya Markiv, Yu. V. Voroshilov and R.V. Skolozdra, Izvest. Akad. Nauk SSSR, Neorg. Mat., 1966, 2, 259 (Tr. Sov. Inorg. Mat., 1966, 2, 222).

90. S. Kass and W.W. Kirk, ASM Trans. Quart., 1962, 55, 77.

91. S. Kass, Bettis Atomic Power Lab., Report WAPD-TM-544 (1966).

92. J.S. Foord, P.J. Goddard and R.M. Lambert, Surf. Sci., 1980, 94, 339.

Note added in Proof

A number of further references appeared in the J. Less Common Metals edition devoted to the Proceedings of the Int. Symp. on the Properties and Applications of Metal Hydrides V. Maubisson, France, May 25-30, 1986 (93-97). Some of these were pertinent to the discussion above. A paper on deuterium absorption in Hf_2Fe (93) showed that a single-phase product could be obtained at low temperature. This supports Aubertin et al. who observed a similar absorption by Zr_2Fe (51), but does not deal any further with effects of oxygen in stabilising these phases and their hydrides against disproportionation. Two other papers (94,95) show a similar phenomenon for Zr_2Ni, but again do not consider the possibility of oxygen stabilisation of the hydride. The final two papers (96,97) on Zr_2Pd also fail to consider the known effects of oxygen in stabilising the hydrides (58).

93. J.L. Soubeyroux, D. Fruchart, S. Derdour, P. Vuillet and A. Rouault, J. Less. Comm. Met., 1987, 129, 187.

94. P. Boyer and A. Baudry, ibid., p. 213.

95. F. Aubertin, S.J. Campbell, J.M. Pope and U. Gonser, ibid., p. 297.

96. A.J. Maeland, E. Lukacevic, J.J. Rush and A. Santoro, ibid., p. 77.

97. F.E. Spada, R.C. Bowman Jr., and J.S. Cantrell, ibid., p. 197.

Table 1

Properties of Zirconium Intermetallic Hydrogen Storage Alloys (Zr-V; Zr-Cr; Zr-Mo Systems)

INTERMETALLIC		HYDRIDE						
Composition	Structure	Max. Comp.	Structure	H:M	ΔH (kcal)	eqm. press. atm(°C)	Precond. treatment	Refs.
ZrV_2	C15;a=7.429;7.442	$ZrV_2H_{5.5}$	C15;a=7.92	1.83	-9.4,10.0	10^{-3}(20°C)	20°C,30-60at	23-25,32
		$ZrV_2D_{6.9}$	C15;a=7.913,7.946	1.63				29,36
Zr_3V_2O	Ti_2Ni;a=12.16	$Zr_3V_2OH_{5.5}$						58,61
Zr_3V_2N	Ti_2Ni;a=12.15	$Zr_3V_2ND_X$	Ti_2Ni;a=12.93	?	-	-	20°C,30at	32
$ZrV_{1.8}Fe_{0.2}$	C15;a=7.396	$ZrV_{1.8}Fe_{0.2}H_{3.6}$	-	1.43	-	-	-	35
$ZrV_{1.67}Fe_{0.33}$	C15;a=7.331	-	-	-	-	$5x10^{-3}$(500°C)	≥350°C	31
$ZrV_{1.5}Fe_{0.5}$	C14;a=5.165, c=8.364	-	-	-	-	~10(400°C)	-	47
$ZrV_{1.2}Fe_{0.8}$	C15;a=1.326	-	-	-	4.7	~10(400°C)		33
$ZrV_{1.3}Fe_{0.7}$	C14;a=5.127, c=8.347	-	-	-	-	~10(400°C)	-	47
ZrVFe	C14;a=5.092, c=8.31		-	1.07	-	-	-	23
$ZrV_{1.5}Co_{0.5}$	C14;a=5.15, c=8.37	$ZrV_{1.5}Co_{0.5}H_{3.2}$	-	1.4	-	-	-	23
$ZrCr_2$	<995°C C14; a=5.107,5.107 c=8.272,8.307	$ZrCr_2H_{4.1}$	-	1.37	-3.3,-11.0	10^{-3}(20°C)	20°C,60at	23-25 34,35
	>995°C C15;a=722	$ZrCr_2D_{3.8}$	C15;a=7.658	1.33	-	-	-	29
$ZrCr_2O_{0.1}$	C14;a=5.08,c=8.28	-	-	-	-	-	-	46
$ZrCr_{1.5}Co_{0.5}$	C14;a=5.05,c=8.28	$ZrCr_{1.5}Co_{0.5}H_{3.25}$	-	1.08	-	-	-	23
ZrCrCo	C14;a=5.034,c=8.22	$ZrCrCoH_{3.2}$	-	1.07	-9.6	0.7(20°C)	-	23
$ZrCr_{1.2}V_{0.8}$	C15;a=7.257	$ZrCr_{1.2}V_{0.8}H_X$	C15;a=7.742	?	-12.7	~10(350°C)	700°C,2at	33
ZrCrV	C15;a=7.281	$ZrCrVH_X$	C15;a=7.759	?	<-12.7	<10(350°C)	700°C,2at	33
$ZrCr_{0.8}V_{1.2}$	C15;a=7.316	$ZrCr_{0.8}V_{1.2}H_X$	C15;a=7.782	?	<-12.7	<10(350°C)	700°C,2at	33
$Zr_{0.75}Ti_{0.25}Cr_2$	C14;a=5.08,c=8.24	$Zr_{0.75}Ti_{0.25}Cr_2H_{3.7}$	-	1.23	-	-	-	35
$Zr_{0.5}Ti_{0.5}Cr_2$	C14;a=5.08,c=8.20	$Zr_{0.5}Ti_{0.5}Cr_2H_{3.25}$	-	1.08	-	-	-	35
$ZrMo_2$	C15;a=7.593	$ZrMo_2H_{0.78}$	-	0.26	-3.6	~10(0°C)	20°C,15at	25

Table 1 (cont.)

Properties of Zirconium Intermetallic Hydrogen Storage Alloys (Zr-Mn System)

INTERMETALLIC		HYDRIDE						
Composition	Structure	Max. Comp.	Structure	H:M	ΔH (kcal)	eqm. press. atm(°C)	Precond. treatment	Refs.
$ZrMn_{1.8}$	C14;a=5.045, c=8.284	$ZrMn_{1.8}H_{2.2}$	C14;a=5.495, c=8.88	0.78	-	-	-	40,44
$ZrMn_2$	C14;a=5.045 8.284; 5.035 8.275; 5.032 8.225; 5.026 8.258	$ZrMn_2H_{3.8}$	C14;a=5.48, c=8.931	1.3	-12.7	-	20°C,60at	23,26 35,40 44
		$ZrMn_2D_3$	C14;a=5.391, c=8.748	1.0	-	-	-	29,36,41
$ZrMn_{2.4}$	C14;a=5.021, c=8.245	$ZrMn_{2.4}H_{3.6}$	C14;a=5.424, c=8.682	1.06	-	-	-	40
$ZrMn_{2.8}$	C14;a=5.004, c=8.208	$ZrMn_{2.8}H_{3.6}$	C14;a=5.415, c=8.817	0.95	-4.3	0.3(30°C)	-	44
$ZrMn_{2.2}$	C14;a=4.987, c=8.202	$ZrMn_{2.2}H_{4.6}$	C14; - -	0.95	-	-	-	40
$ZrMn_{2.8}$	C14;a=4.957, c=8.088	$ZrMn_{2.8}H_{3.6}$	C14;a=5.386, c=8.799	0.75	-4.8	0.5(30°C)	-	44
$Zr_{0.8}Ti_{0.2}Mn_2$	C14;a=5.01, c=8.23	-	-	1.16	-	-	20°C,70at	35
$Zr_{0.8}Ti_{0.2}MnFe$	C14;a=4.98, c=8.163	$Zr_{0.8}Ti_{0.2}MnFeH_{3.0}$	C14;a=5.284,c=8.628	1.0	-2.9	-1(23°C)	-	48
$Zr_{0.7}Ti_{0.3}MnFe$	C14;a=4.958, c=8.628	$Zr_{0.7}Ti_{0.3}MnFeH_{2.0}$	C14;a=5.271,c=8.623	0.66	-2.4	-2(23°C)	-	41
$Zr_{0.6}Ti_{0.4}Mn_2$	C14;a=4.98, c=8.21	$Zr_{0.6}Ti_{0.4}Mn_2H_{3.3}$	-	1.1	-	8(140°C)	20°C,70at	26,35
$Zr_{0.5}Ti_{0.5}Mn_{1.35}Fe_{0.35}$	C14; -	-	-	-	-	-1(140°C)	-	42
$ZrMn_{1.6}Fe_{0.4}$	C14;a=5.022 8.207; 5.03,c=8.243	$ZrMn_{1.6}Fe_{0.4}H_{3.5}$	C14;a=5.467, c=8.908	1.2	-	-	-	37,38
$ZrMn_{1.3}Fe_{0.7}$	C14;a=5.022,c=8.215	$ZrMn_{1.3}Fe_{0.7}H_{3.6}$	C14;a=5.461, c=8.892	1.2	-	-	-	38
$ZrMn_{1.2}Fe_{0.8}$	C14;a= 5.012, c= 8.188	$ZrMn_{1.2}Fe_{0.8}H_{3.2}$	-	1.07	-7.9	0.4(20°C)	-	23
					-7.2			23
ZrMnFe	C14;a=5.006 8.178; 5.008, c=8.182; 5.011 8.202	$ZrMnFeH_{3.5}$	C14;a=5.69 7.516; 5.422, c=8.839	1.17	-18,-8.2	0.2-0.65(25°C)	-	38,43
$ZrMnFe_{1.2}$	C14;a=4.996, c=8.173	$ZrMnFe_{1.2}H_{3.2}$	C14;a=5.205, c=8.685	1.0	7.5	-1(23°C)	-	39
$ZrMnFe_{1.3}$	C14;a=4.988, c=8.163	$ZrMnFe_{1.3}H_{3.6}$	C14;a=5.184, c=8.618	0.79	6.8	-3(23°C)	-	39
$ZrMnFe_{1.4}$	C14;a=4.990, c=8.178	$ZrMnFe_{1.4}H_{0.15}$	-	0.1	-	-	-	39
$ZrMnFeCr_{0.25}$	C14;a=5.014, c=8.196	$ZrMnFeCr_{0.25}H_{3.6}$	-	1.11	6.1	-1(65°C)	-	37
ZrMnCr	C14;a= 5.07, c= 8.323	-	-	-	-	-	-	37
$Zr_{0.8}Ti_{0.2}MnCr_{1.25}$	C14;a=4.998, c=8.236	$Zr_{0.8}Ti_{0.2}MnCr_{1.25}H_{3.7}$	-	1.14	-	-	-	37
$ZrMnFeCo_{0.4}$	C14;a=4.984, c=8.134	$ZrMnFeCo_{0.4}H_{0.01}$	-	0.003	-	-	-	37
$ZrMnFeNi_{0.4}$	C14;a=4.992, c=8.153	$ZrMnFeNi_{0.4}H_{1.7}$	-	0.5	-	-	-	37
$ZrMn_{1.3}Co_{0.5}$	C15;a=7.09	$ZrMn_{1.3}Co_{0.5}H_{3.4}$	-	1.13	-10.6	0.08(25°C)	-	23
$ZrMn_{1.2}Co_{0.8}$	C14;a=5.00, c=8.19	$ZrMn_{1.2}Co_{0.8}H_{3.1}$	-	1.03	-8.6	0.5(25°C)	-	23
ZrMnCo	C15;a=7.085; C14;a= 5.00, c= 8.16; 5.00 8.16	$ZrMnCoH_{3.1}$	-	1.03	-8.3	1.2(25°C)	-	53,23

Table 1 (cont.)

Properties of Zirconium Intermetallic Hydrogen Storage Alloys (Zr-Fe(Cr) System)

INTERMETALLIC		HYDRIDE						
Composition	Structure	Max. Comp.	Structure	H:M	ΔH (kcal)	eqm. press. atm(°C)	Precond. treatment	Refs.
$Zr_{7.4}Fe_{26}$	amorphous	$Zr_{7.4}Fe_{26}H_{23.8}$	-	2.38	-	-	-	50
Zr_3Fe	Re_3Ba-3.32, b-10.95,c-8.81	$Zr_{7.5}Fe_{23.5}H_{17.8}$	disproportionates?	1.78	-	-	-	50
Zr_2Fe	Ti_2Ni;a=11.7, or C16	$ZrFe_2$+ZrH_2 (at T ≥ 400°C)	disproportionates	-			≥450°C	31,51
$Zr_{9}Fe_2O_{0.6}$	Ti_2Ni;a=11.8	$Zr_{9}Fe_2O_{0.6}H_{5.4}$	Ti_2Ni	0.82	-	-	-	51,52
$ZrFe_2$	C15;a=7.064	$ZrFe_2H_{0.12+}$+ZrH_2	disproportionates	0.2	-8.0	-	20°C,60atm	23
$ZrFe_{1.6}Cr_{0.4}O_{0.04}$	C14;a=4.97, c=8.15	-		0.85	-	-	-	46
$ZrFe_{1.5}Cr_{0.5}$	C14;a=5.02, c=8.19	$ZrFe_{1.5}Cr_{0.5}H_{2.85}$		0.93	-5.8	55(25°C)	-	23
$ZrFe_{1.5}Cr_{0.5}O_{0.5}$	C14;a=5.00, c=8.165	-		1.00	-6.6	-	-	46
$ZrFe_{1.4}Cr_{0.6}$	C14;a=5.006, c=8.196	$ZrFe_{1.4}Cr_{0.6}H_{3.1}$	C14;a=5.327,c=8.701	1.03	-6.9	0.6(23°C)	-	45
$ZrFe_{1.4}Cr_{0.6}O_{0.04}$	C14;a=5.005, c=8.175	-		-	-6.0	-	-	46
$Zr_{0.8}Ti_{0.2}Fe_{1.4}Cr_{0.6}$	C14;a=4.981,c=8.146	$Zr_{0.8}Ti_{0.2}Fe_{1.4}Cr_{0.6}H_{3.0}$	C14;a=5.318,c=8.667	1.00	-6.4	3(23°C)	-	45
$Zr_{0.7}Ti_{0.3}Fe_{1.4}Cr_{0.6}$	C14;a=4.970, c=8.173	$Zr_{0.7}Ti_{0.3}Fe_{1.4}Cr_{0.6}H_{2.7}$	C14;a=5.310, c=8.656	0.9	-5.2	6(23°C)	-	45
$ZrFe_{1.3}Cr_{0.7}O_{0.04}$	C14;a=5.005, c=8.190	-		-	-	-	-	46
$Zr_{0.8}Ti_{0.2}Fe_{1.3}Cr_{0.7}$	C14;a=4.991, c=8.174	$Zr_{0.8}Ti_{0.2}Fe_{1.3}Cr_{0.7}H_{2.95}$	C14;a=5.299, C=8.699	0.98	-	-	-	45
$ZrFe_{1.2}Cr_{0.8}$	C14;a=5.02, c=8.22 C15;a=7.01	$ZrFe_{1.2}Cr_{0.8}H_{1.5}$	-	0.5	-	-	300°C	53
$ZrFe_{1.1}Cr_{0.9}O_{0.07}$	C14;a=5.02; c=8.235	-	-	-	-	-	-	46
	C14;a=5.029 c=8.241 5.034 c=8.220 5.045 c=8.200				-8.7	0.2(51°C)	-	49
		$ZrFeCrH_{3.3}$	C14;a=5.346, c=8.707	1.10	-11.5	10^{-3}(25°C)	-	23
ZrFeCr	C15;a=7.12							
$ZrFe_{0.8}Cr_{1.2}$	C14;a=5.05, c=8.26 C15;a=7.20	$ZrFe_{0.8}Cr_{1.2}H_{2.8}$	-	0.93	-	-	300°C	53
$ZrFe_{0.9}Cr_{1.1}O_{0.07}$	C14;a=5.025, C=8.245	$ZrFe_{0.9}Cr_{1.1}O_{0.07}H_{2.9}$	-	0.95	-	-	-	53,46
$ZrFe_{0.5}Cr_{1.5}$	C14;a=5.062, C=8.267	$ZrFe_{0.5}Cr_{1.5}H_{3.4}$	-	1.13	-11.8	0.1(25°C)	-	23
$ZrFe_{0.5}Cr_{1.5}O_{0.05}$	C14;a=5.04, c=8.275	-	-	-	-	-	-	46
$Zr_{0.7}Ti_{0.3}FeCr$	C14;a=4.983, c=8.179	$Zr_{0.7}Ti_{0.3}FeCrH_{3.2}$	C14;a=5.308, c=8.631	1.07	-6.7	-1(23°C)	-	49
$Zr_{0.5}Ti_{0.5}FeCr$	C14;a=4.950, c=8.101	$Zr_{0.5}Ti_{0.5}FeCrH_{3.7}$	C14;a=5.211, c=8.534	0.9	-5.8	-10(23°C)	-	49
$ZrFe_{1.4}Cr$	C14;a=5.007, c=8.194	$ZrFe_{1.4}CrH_{3.6}$	-	1.12	-4.9	-1(25°C)	-	37
$ZrFe_{1.5}Cr$	C14;a=5.003. c=8.169	$ZrFe_{1.5}CrH_{3.4}$	-	0.97	-5.4	-2(25°C)	-	37
$ZrFe_{1.6}V_{0.2}$	C15;a=7.085	$ZrFe_{1.6}V_{0.2}H_{1.4}$	-	0.53	-	-	-	35
$ZrFe_{1.6}V_{0.4}$	C14;a=5.02, c=8.21	$ZrFe_{1.6}V_{0.4}H_{2.9}$	-	0.97	-	-	-	35
$ZrFe_{1.5}V_{0.5}$	C14;a=5.036, c=8.225	$ZrFe_{1.5}V_{0.5}H_{3.2}$	-	1.07	-7.7	0.25(25°C)	≥350°C	23,31
$ZrFe_{1.8}Mn_{0.2}$	C15;a=7.065	$ZrFe_{1.8}Mn_{0.2}H_{0.2}$	-	0.07	-	-	-	35
$ZrFe_{1.8}Mn_{0.4}$	C15;a=7.067	$ZrFe_{1.8}Mn_{0.4}H_{0.2}$	-	0.07	-	-	-	35
$ZrFe_{1.5}Mn_{0.5}$	C15;a=7.09	$ZrFe_{1.5}Mn_{0.5}H_{0.44}$	-	0.15	-	-	-	35
$ZrFe_{1.2}Mn_{0.8}$	C14;a= 5.00 c=8.17 5.00 c=8.17 C15;a=6.93	$ZrFe_{1.2}Mn_{0.8}H_{2.0}$	-	0.66	-	-	-	53,35
$ZrFe_{1.83}Al_{0.17}$	C15;a=7.091	$ZrFe_{1.83}Al_{0.17}H_{0.8}$	-	0.27	-	25(25°C)	-	30
$ZrFe_{1.66}Al_{0.33}$	C15;a=7.124	$ZrFe_{1.66}Al_{0.33}H_{2.2}$	-	0.73	-	7(25°C)	-	30
$ZrFe_{1.6}Al_{0.4}$	C15;a=7.126	$ZrFe_{1.6}Al_{0.4}H_{2.7}$	-	0.73	-	3(25°C)	-	30
$ZrFe_{1.5}Al_{0.5}$	C15;a=7.129 C14;a=5.063, c=8.252	$ZrFe_{1.5}Al_{0.5}H_{2.0}$	-	0.66	-	0.1(25°C)	-	30

Table 1 (cont.)

Properties of Zirconium Intermetallic Hydrogen Storage Alloys (Zr-Co,Zr-Ni,Zr-Cu,Zr-Al,Zr-Pd Systems)

INTERMETALLIC		HYDRIDE						
Composition	Structure	Max. Comp.	Structure	H:M	ΔH (kcal)	eqm. press. atm(°C)	Precond. treatment	Refs.
ZrCo	CsCl;a=3.196	$ZrCoD_3$ $ZrCoH_{2.6}$	a=3.53,b=10.48,c=4.30 a=3.441,b=10.268, c=4.19	1.5 1.3	- -18.0	- 10^{-3}(150°C)	- -	55,54 27
$ZrCo_2$	C15;a=6.952	$ZrCo_2+ZrH_2$	-	0.2	-13.7	-	20°C,60at	23
$ZrCo_{1.6}Cr_{0.4}$	C15;a=6.99	$ZrCo_{1.6}Cr_{0.4}H_{0.3}$	-	0.1	-	-	-	23
$ZrCo_{1.5}Cr_{0.5}$	C15;a=7.02	$ZrCo_{1.5}Cr_{0.5}H_{1.6}$	-	0.53	-	-	-	23
$ZrCo_{1.2}Cr_{0.8}$	C15;a=7.07 C14;a=5.025,c=8.180	$ZrCo_{1.2}Cr_{0.8}H_{1.1}$	-	0.37	-	-	-	53
ZrCoCr	C15;a=7.07 5.034 8.22 C14;a= 5.01 c= 8.18	$ZrCoCrH_{3.2}$	-	1.07	-	-	-	23,53
$ZrCo_{1.5}V_{0.5}$	C14;a=5.00, c=8.16	$ZrCo_{1.5}V_{0.5}H_{3.0}$	-	1.0	-8.2	1.5(25°C)	-	23
ZrCoV	C14;a=5.07, c=8.26	$ZrCoVH_{3.7}$	-	1.23	-11.8	2.10^{-3}(25°C)	-	23
$ZrCo_{1.2}Mn_{0.8}$	C14;a=4.97, c=8.14	$ZrCo_{1.2}Mn_{0.8}H_{0.24}$	-	0.08	-	-	-	53
Zr_2Ni	C16	$ZrNiH_3+ZrH_2$	disproportionates	1.6	-	10^{-3}(500°C)	-	34
ZrNi	CsCl;a=6.98 a=3.26,b=9.94,c=4.09	$ZrNiH_3$	CsCl;a=7.40 a=3.53,b=10.48,c=4.30	1.47	-18.4	10^{-3}(100°C)	-	28,34 57,56
		$ZrNiD_3$	a=3.51,b=10.44,c=4.30	1.7	-	-	-	57,56
Zr_7Ni_{10}	orthorhombic	$Zr_7Ni_{10}H_{17}$	-	1.0	-	-	-	34
Zr_2Cu	$MoSi_2$;a=3.22,c=11.18	$ZrCu_{1.0}+ZrH_2$	disproportionates	0.62	-	10^{-3}(500°C)	-	59,58,34
$ZrAl_2$	C14;a=5.271,c=8.758	$ZrAl_2H_{0.5}$	-	0.17	-17.9	<0.1(25°C),	700°C,60at	30
Zr_4Pd_2O	Ti_2Ni;a=12.458	$Zr_4Pd_2OH_{4.7}$	Ti_2Ni;a=12.60	0.67	-	-	-	58
Zr_2Pd	$MoSi_2$;a=3.306,c=10.894	$Zr_2PdH_{2.7}$	-	0.9	-	-	-	60,58
$ZrPd_2$	$MoSi_2$;a=3.426,c=8.644	-	-	-	-	-	-	58

Footnote: - designation of crystal structures: - C14 - hexagonal c.p. ($MgZr_2$ type)
- C15 - cubic c.p. ($MgCu_2$ type)
- C16 - body centred tetragonal ($CuAl_2$ type)

Table 2

Analyses of Intermetallic Particles in the Zircaloys

Alloy Heat Treatment	$Zr/Ce/Cr)_2$ Phase		$Zr_2(Fe/Ni)$ Phase		Other Phases	Ref.
	Cell Dimensions	Fe:Cr Ratio	Cell Dimensions	Fe:Cr Ratio		
Zircaloy-2	-	-	-	~1	-	67
"	C14?	-	C16;a=6.5, c=5.5	-	hydrides	68
"	C14;a=5.10, c=8.30	0.82	C16;a=6.51, c=5.30	1.5	-	69
"	C14;a=5.01, c=8.22 / C15;a=7.19	-	-	-	-	73
" Standard A	0.4-0.55(C15), rem. C14	0.85-0.9	C16	1.0-1.05	-	77
" Standard B	100%C14	0.80	C16	0.78	-	77
" B-Q	0.99(C15)0.01(C14)	1.75-1.8	C16	1.30-1.35	-	
"	C14	0.78-0.96	C16	1.0-1.5	-	79
"	C14;a=5.10,c=8.40	1.2-1.5	C16;a=6.7, c=5.4	1.2-1.5	-	80
"	C14;a=5.04, c=8.16	0.66	C16;a=6.51, c=5.41	~1.0	-	81
" α-Ann.	C14;a=5.08, c=8.28	0.82	C16;a=6.50, c=5.30	~1.5	β-Sn	82
" β-Quench	C15;a=7.21	-	-		ZrSn	
Zircaloy-4	C14;a=5.079, c=8.279	~2.5	-	-	-	70
"	C14	-	-	-	Zr_2Fe?	71
"	C14 / C15 polytype structure	-	-	-	$ZrSi_2$	72
"	C14;a=5.04, c=8.26	~1.2	-	-	-	74
"	C15;a=7.14, infrequent	-				
"	C14	1.5-3.0	(including Ni,Cu,Si impurities)		-	75
"	C14 / C15 polytype structure	-	-	-	-	76
" α-Ann.	-	1.0-1.7	-	-	Zr_2Fe?	78
" β-Q	-	0.9-1.7	-	-	-	78
"	C14+C15	1.63-1.96	-	-	Zr_2Fe	79
" α-Ann.	C14;a=5.10, c=8.50	2	C16;a=6.4, c=5.5		-	80
" α-Ann.	C14;a=5.04, c=8.16	1.5	C16;a=6.51, c=5.41	5.7	$ZrSi_2$	81
" β-Ann.	C15;a=7.07	2.33	-	-		
" α-Ann.	C14;a=5.08, c=8.28	2.45	-	-	-	83
" (α+β)Qu.	C15;a=7.21	-	-	-	βSn	83

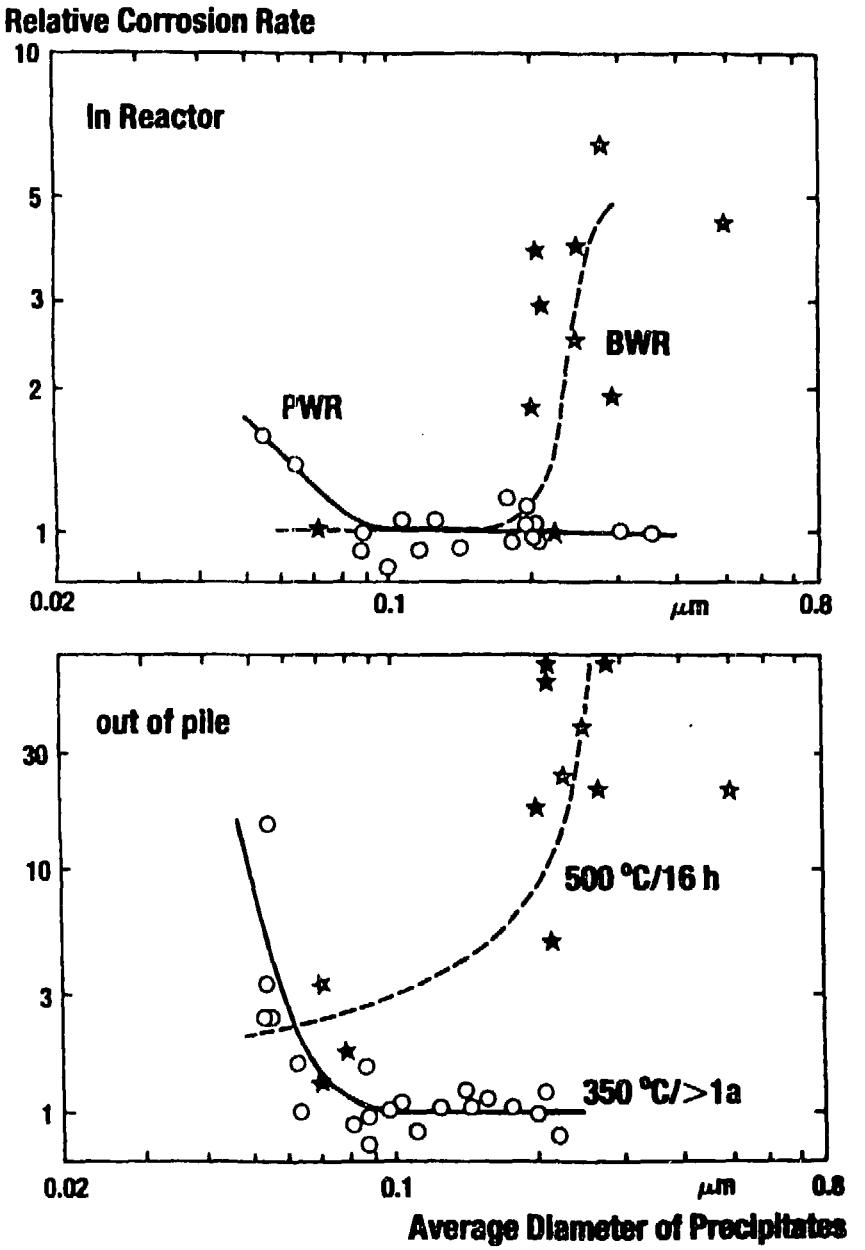

Figure 1: Corrosion of Zircaloy vs. size of intermetallic precipitates. (Ref. 5).

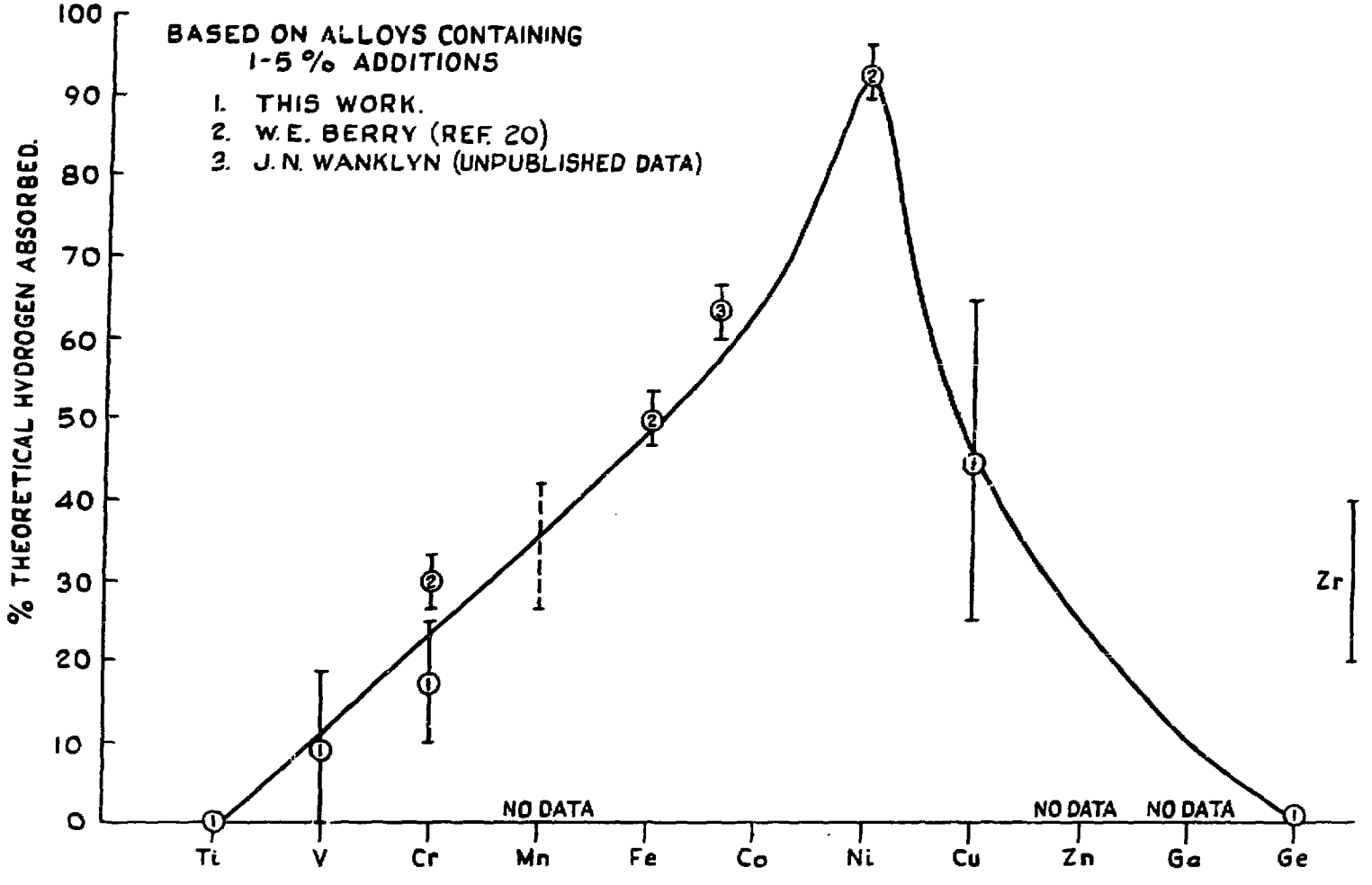

Figure 2: Effect of alloying elements on hydrogen absorption. (Ref. 3).

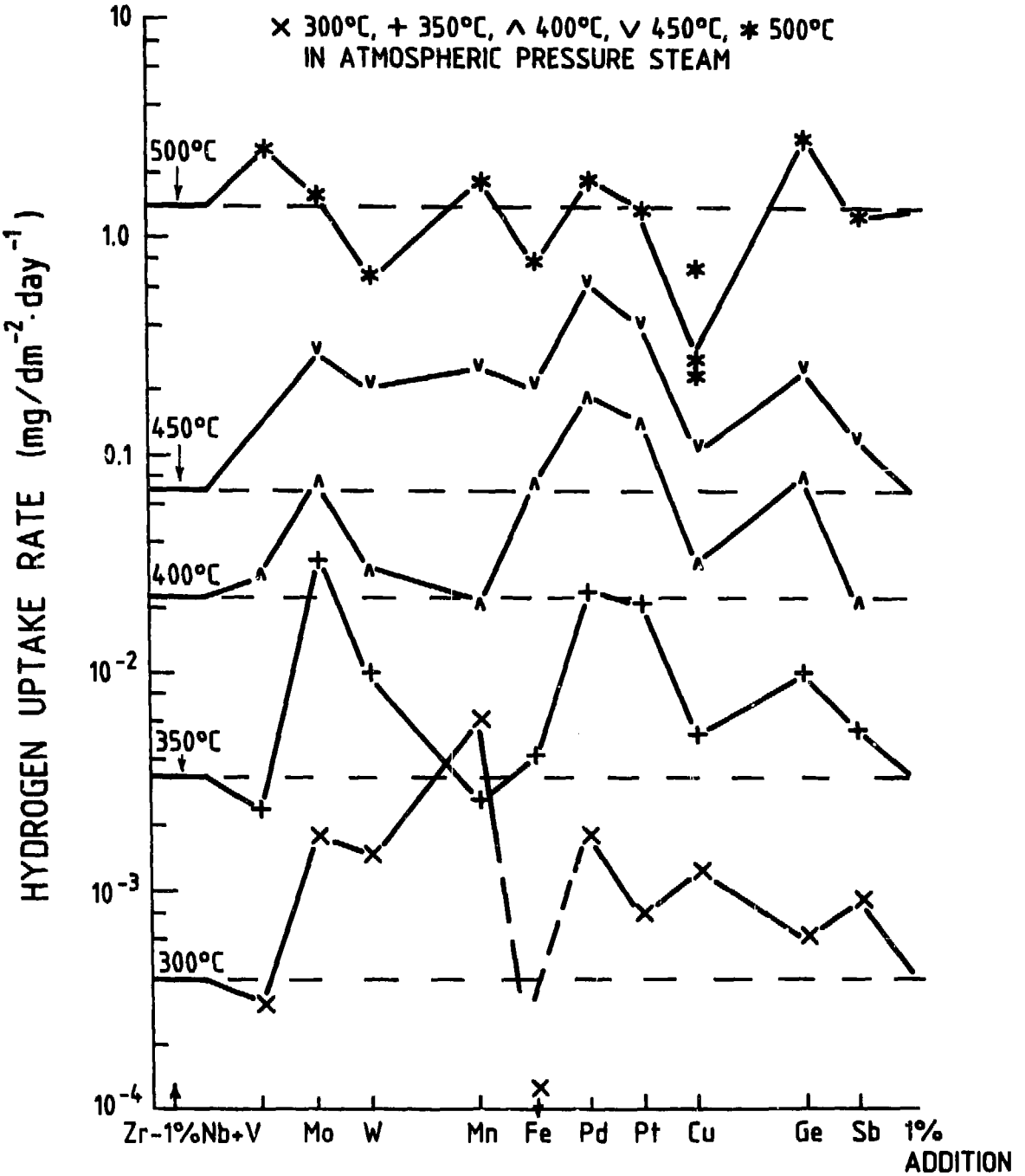

Figure 3a: Effect of ternary additions to Zr-1%Nb on hydrogen uptake rates.

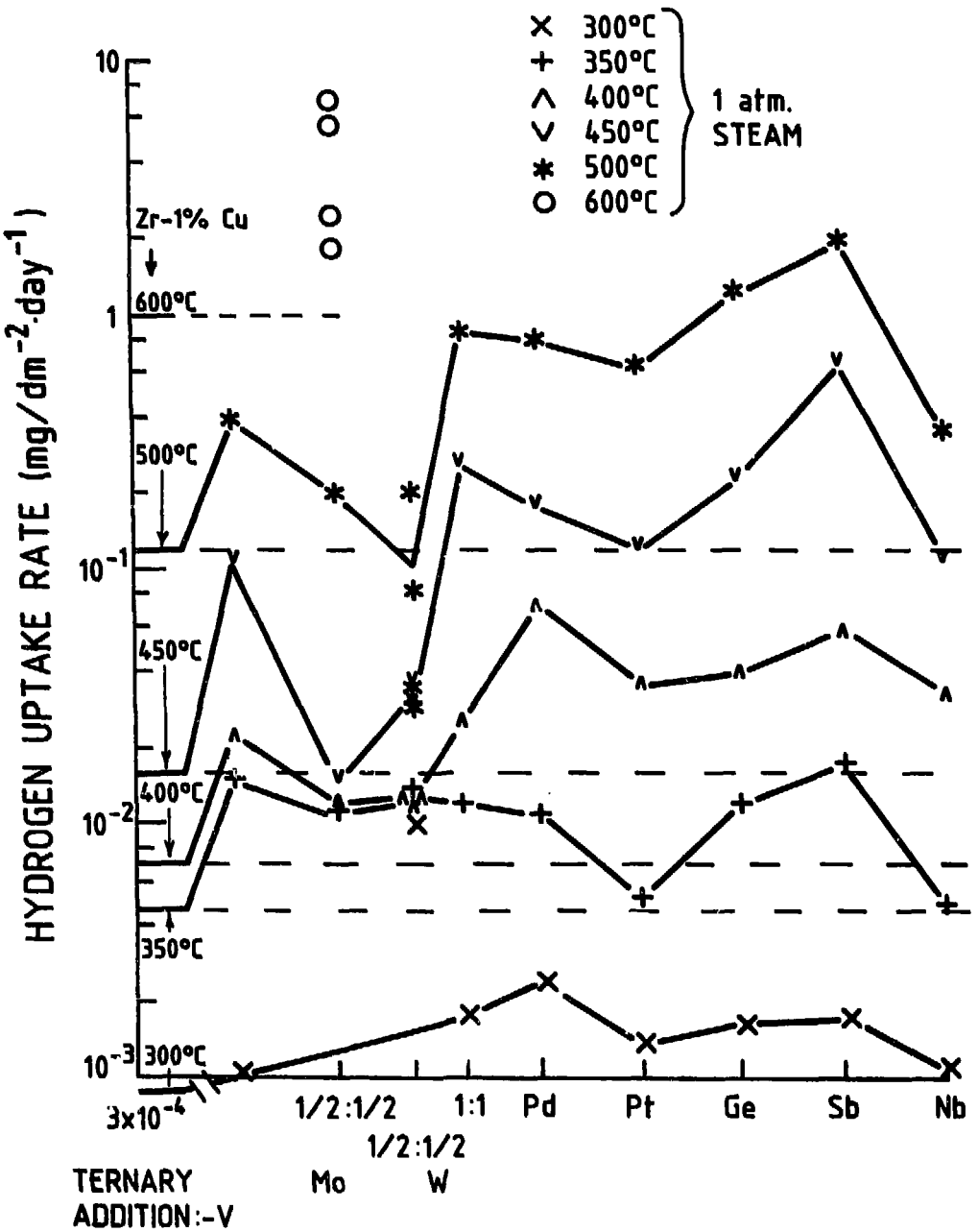

Figure 3b: Effect of ternary additions to Zr-1%Cu on hydrogen uptake.

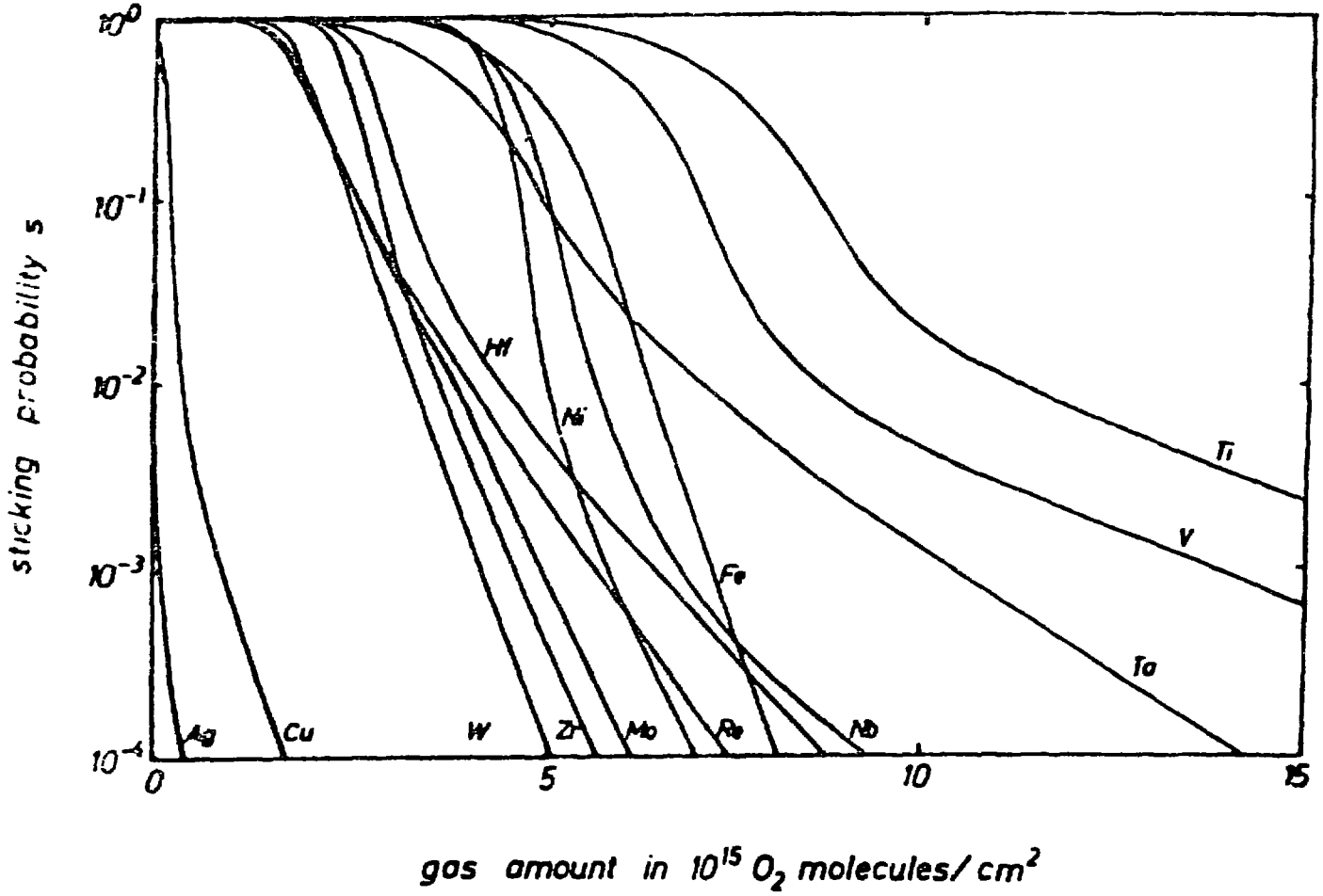

Figure 4: Sticking probability(s) of O_2 on transition metal films at 300 K. A monolayer of oxygen on zirconium is ~1.1 x 10^{15} molecules/cm^2. (Ref. 12).

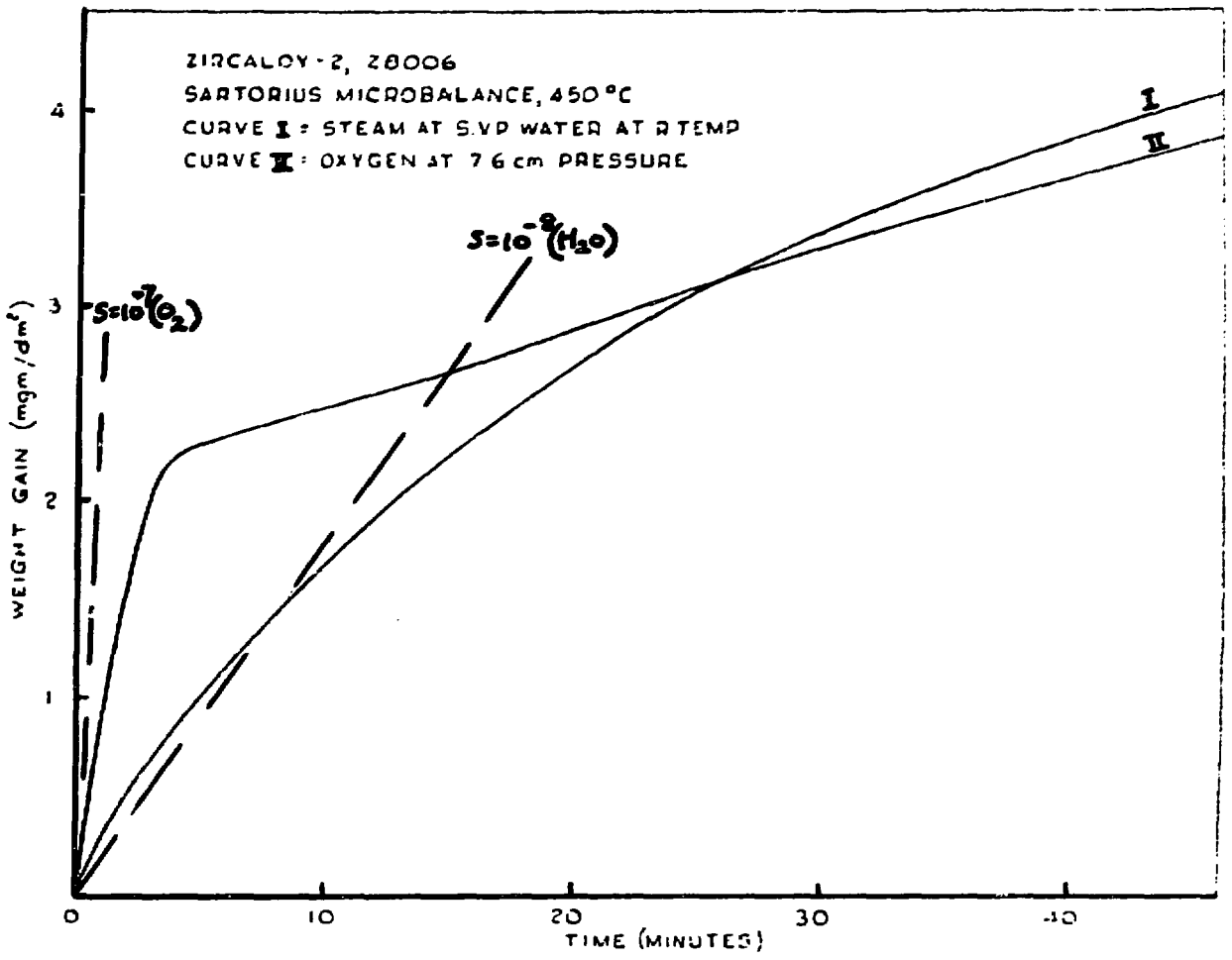

Figure 5: Initial oxidation rates in steam and oxygen. (Ref. 15).

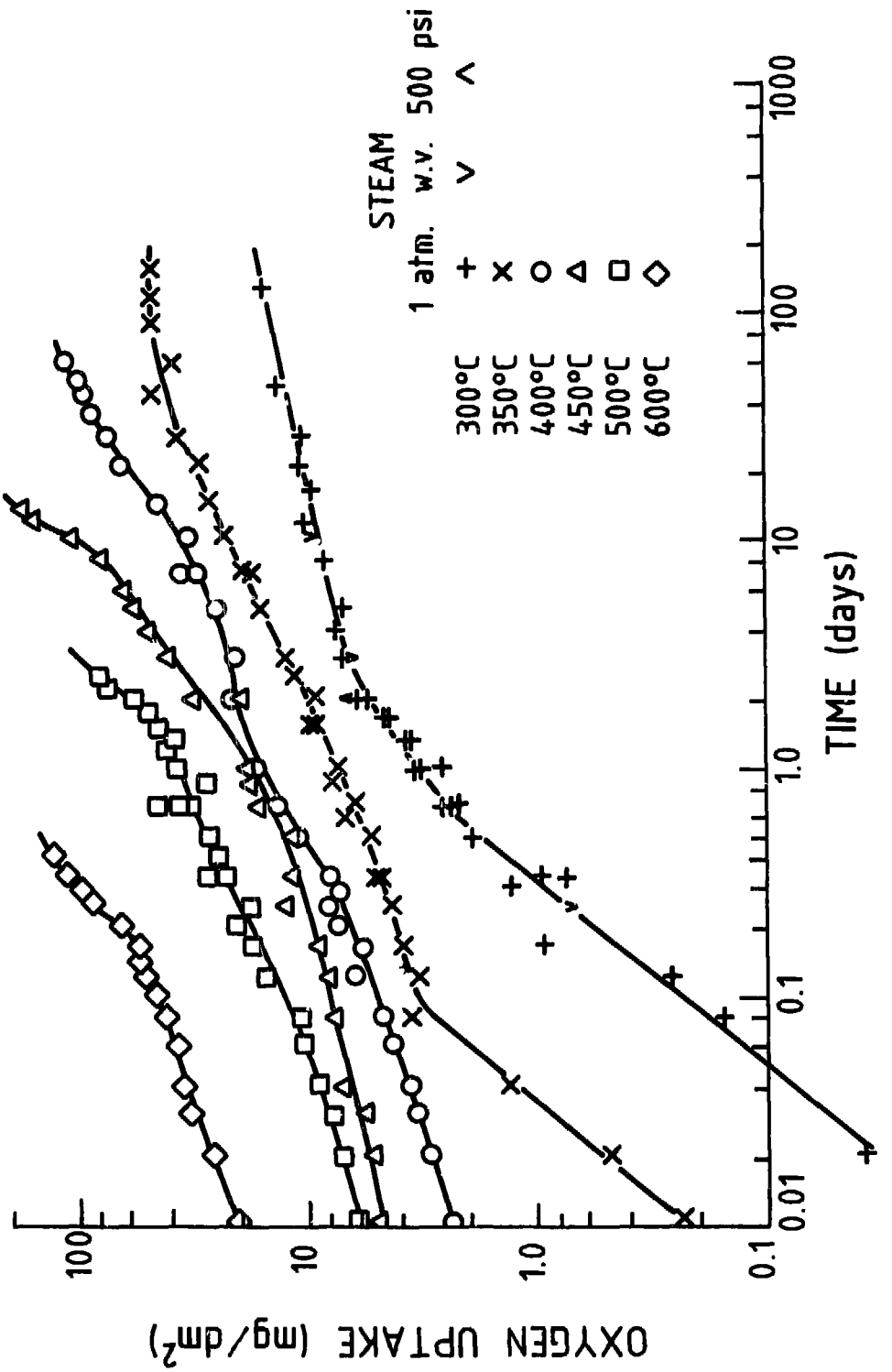

Figure 6: Zircaloy-2 (I.C.I. 0.005" sheet) oxidation in atmospheric pressure steam.

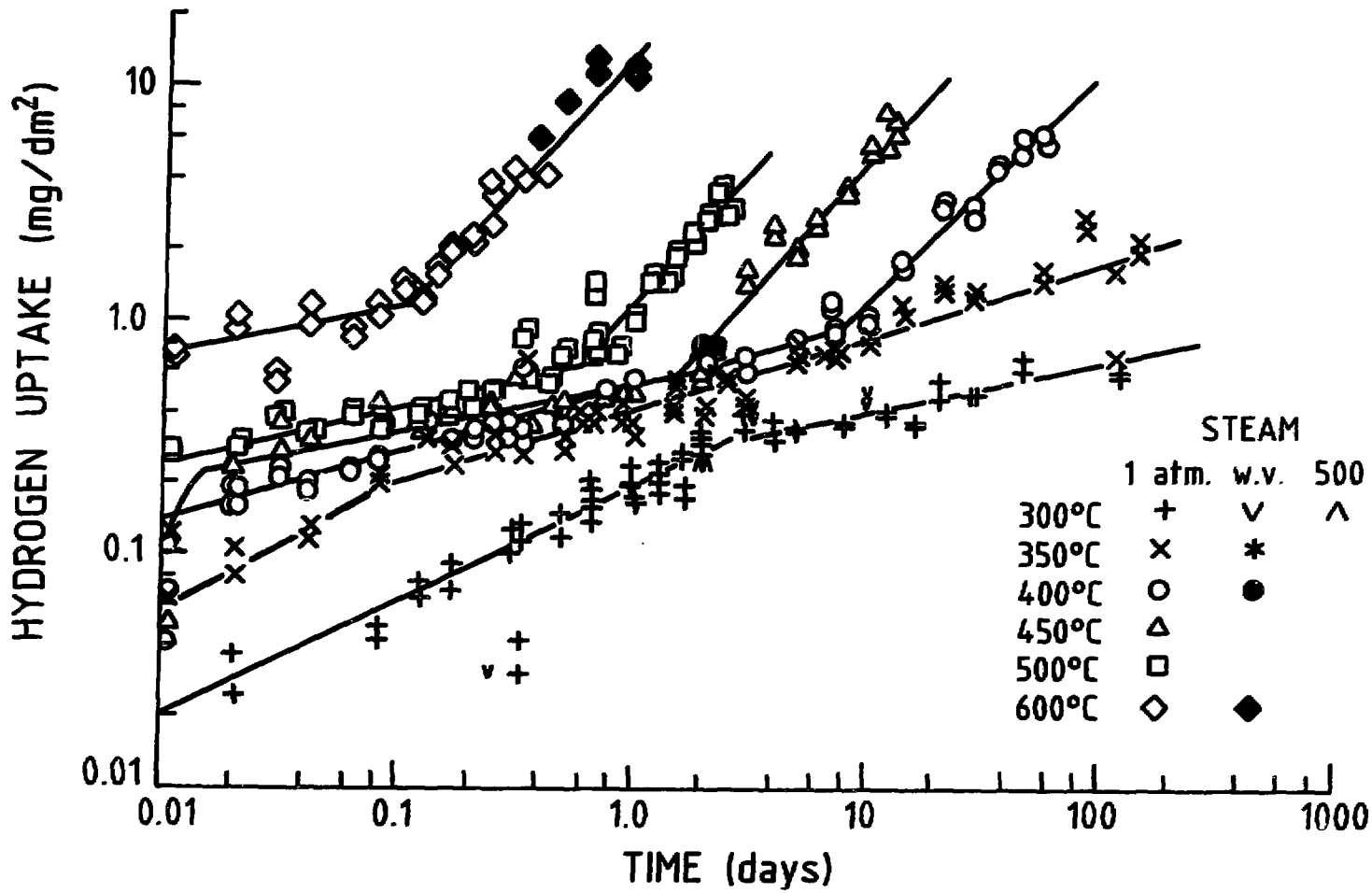

Figure 7: Zircaloy-2 (I.C.I. 0.005" sheet) hydrogen uptake versus time in 1 atm. steam.

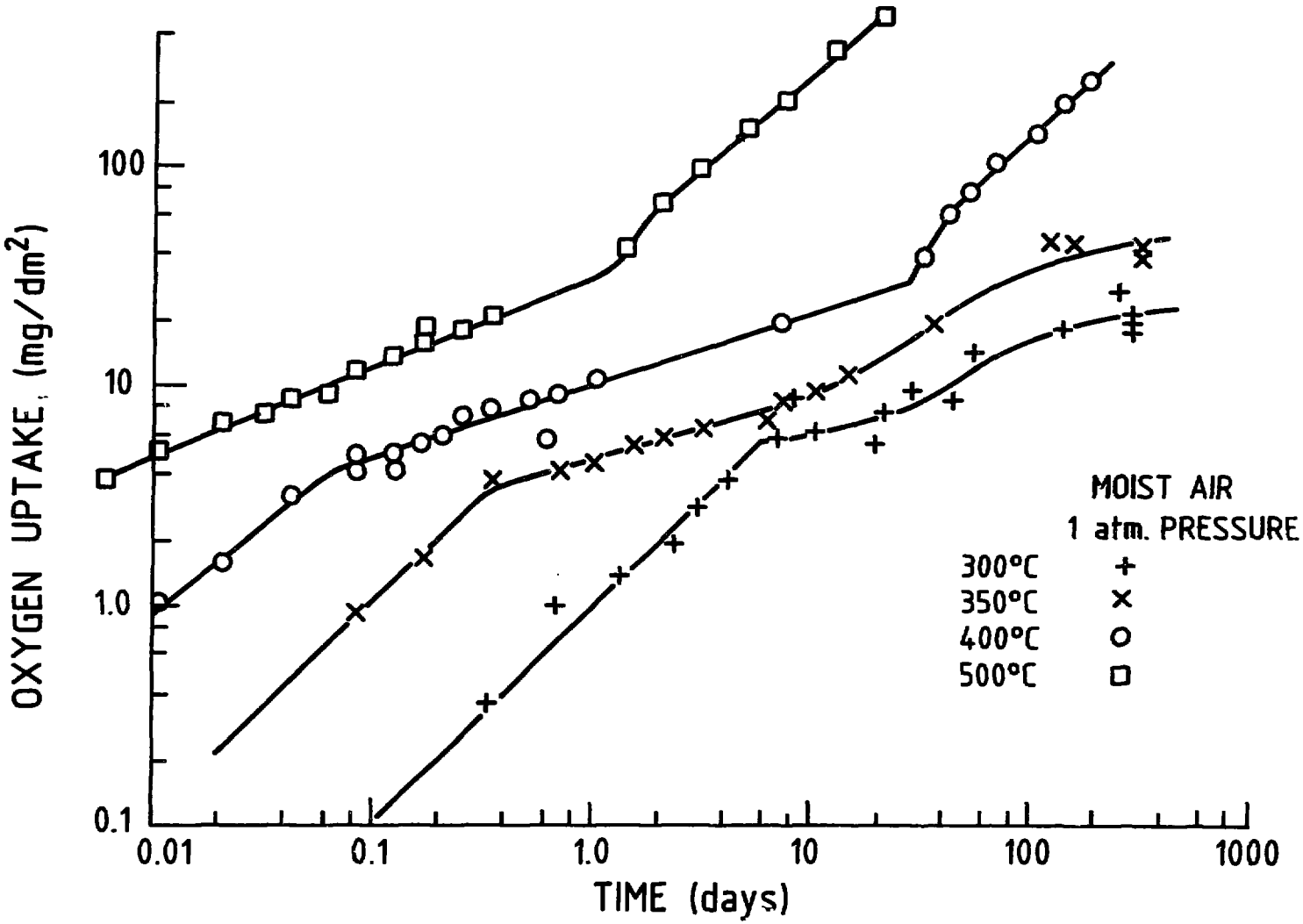

Figure 8: Zircaloy-2 (I.C.I. 0.005" sheet) oxidation in moist air.

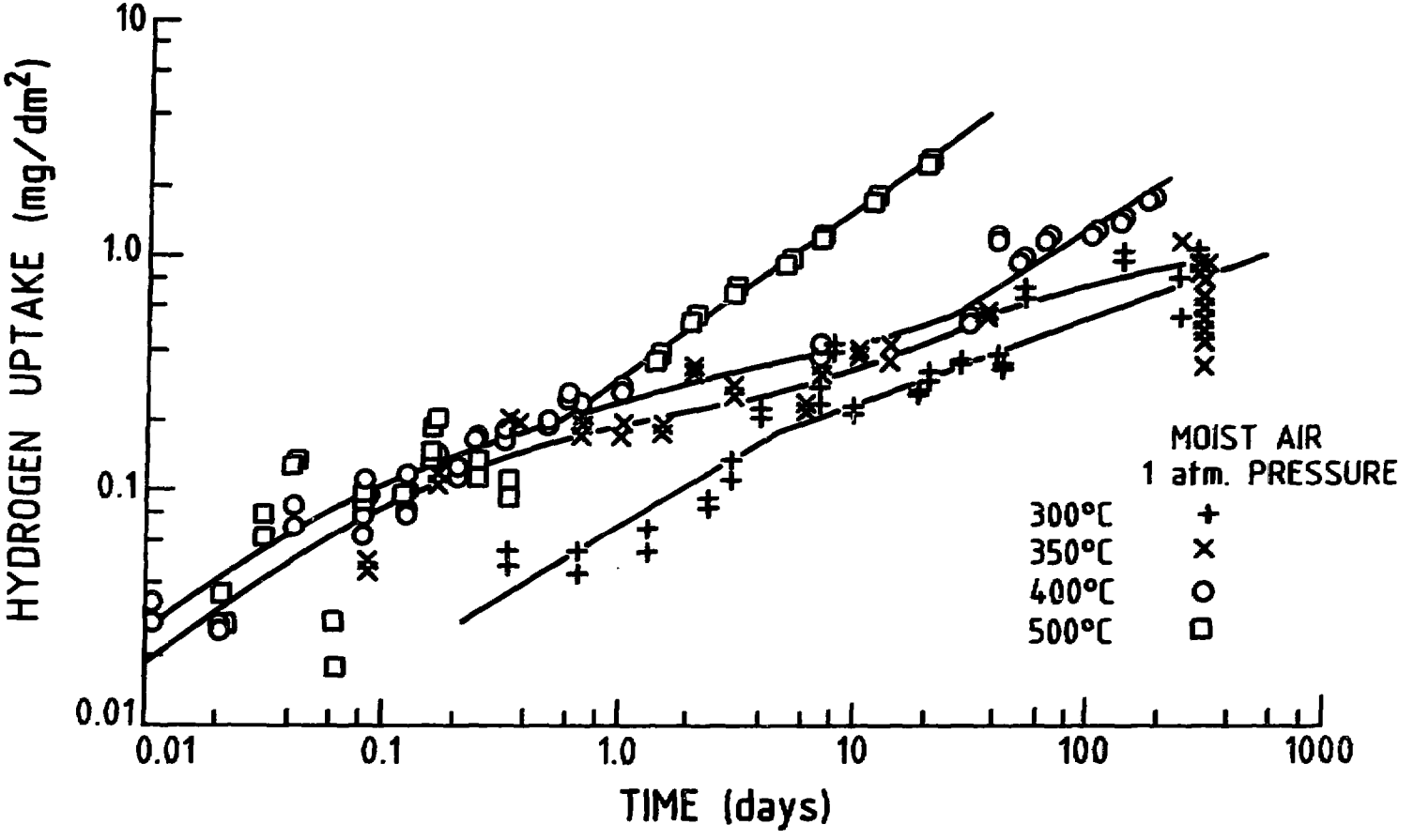

Figure 9: Zircaloy-2 (I.C.I. 0.005" sheet) hydrogen uptake versus time in moist air.

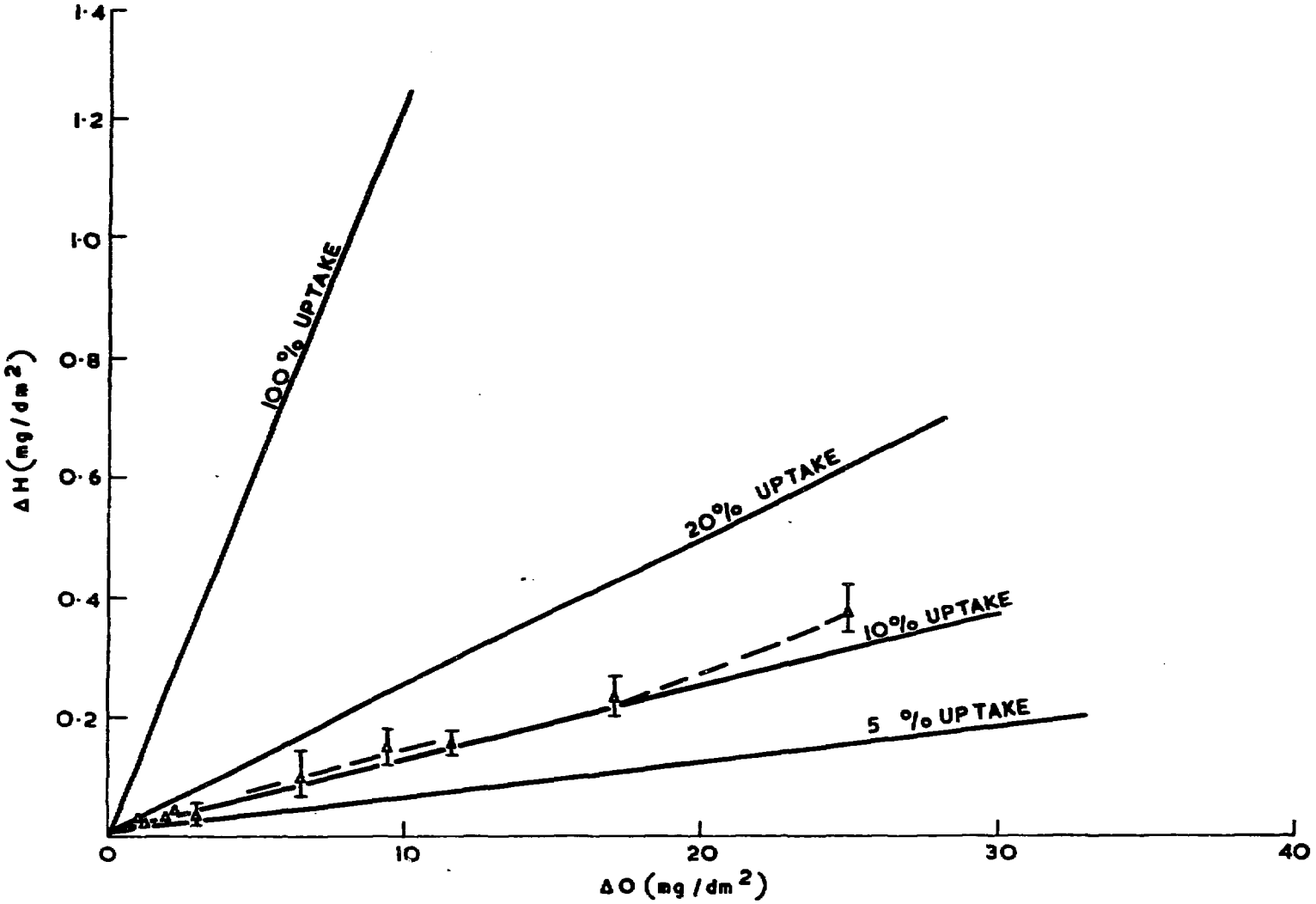

Figure 10: Hydrogen uptake of van Arkel zirconium in steam at 500°C, 1 atm. (Ref. 20).

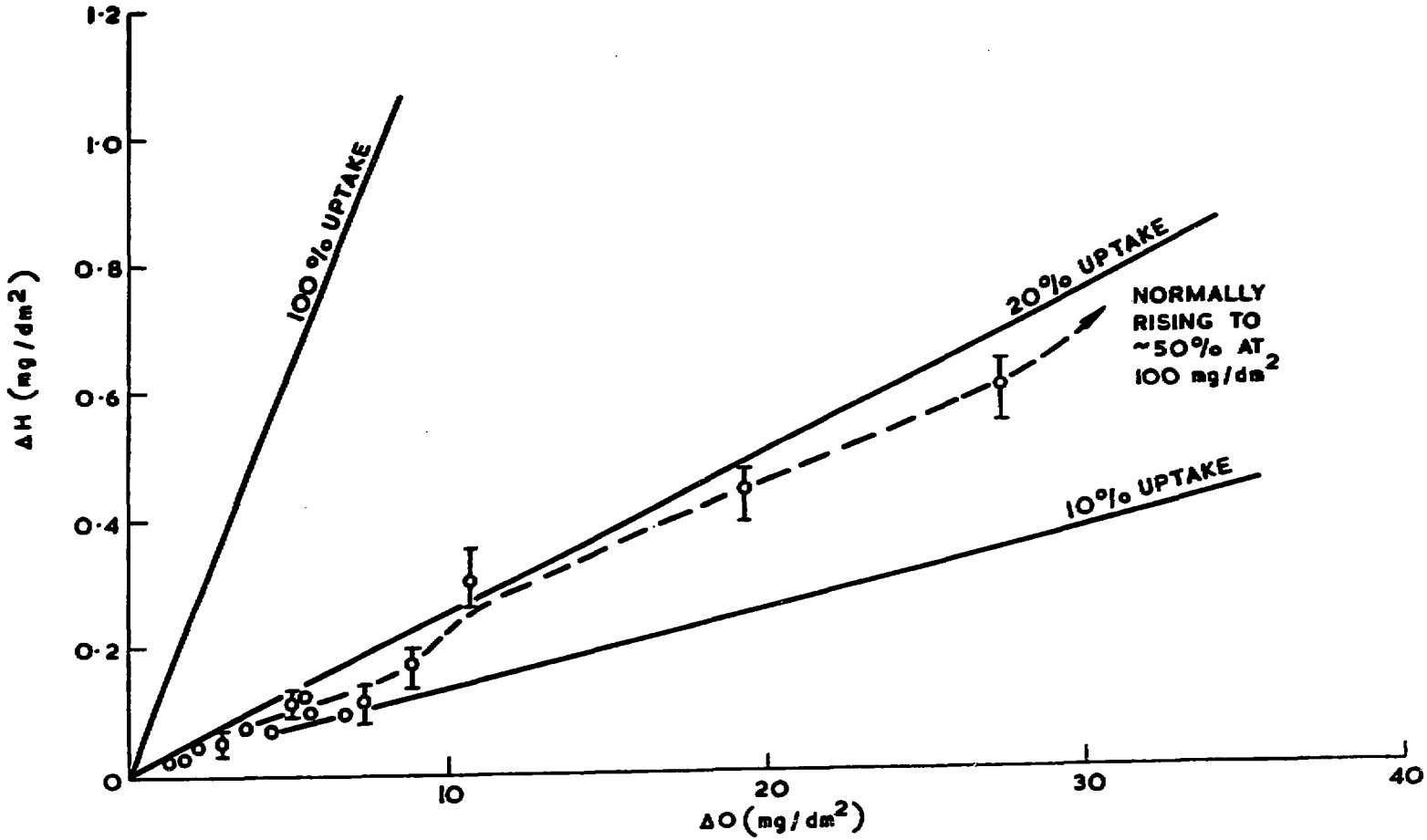

Figure 11: Hydrogen uptake of Zr - 1%Cu in steam at 500°C, 1 atm. (Ref. 20).

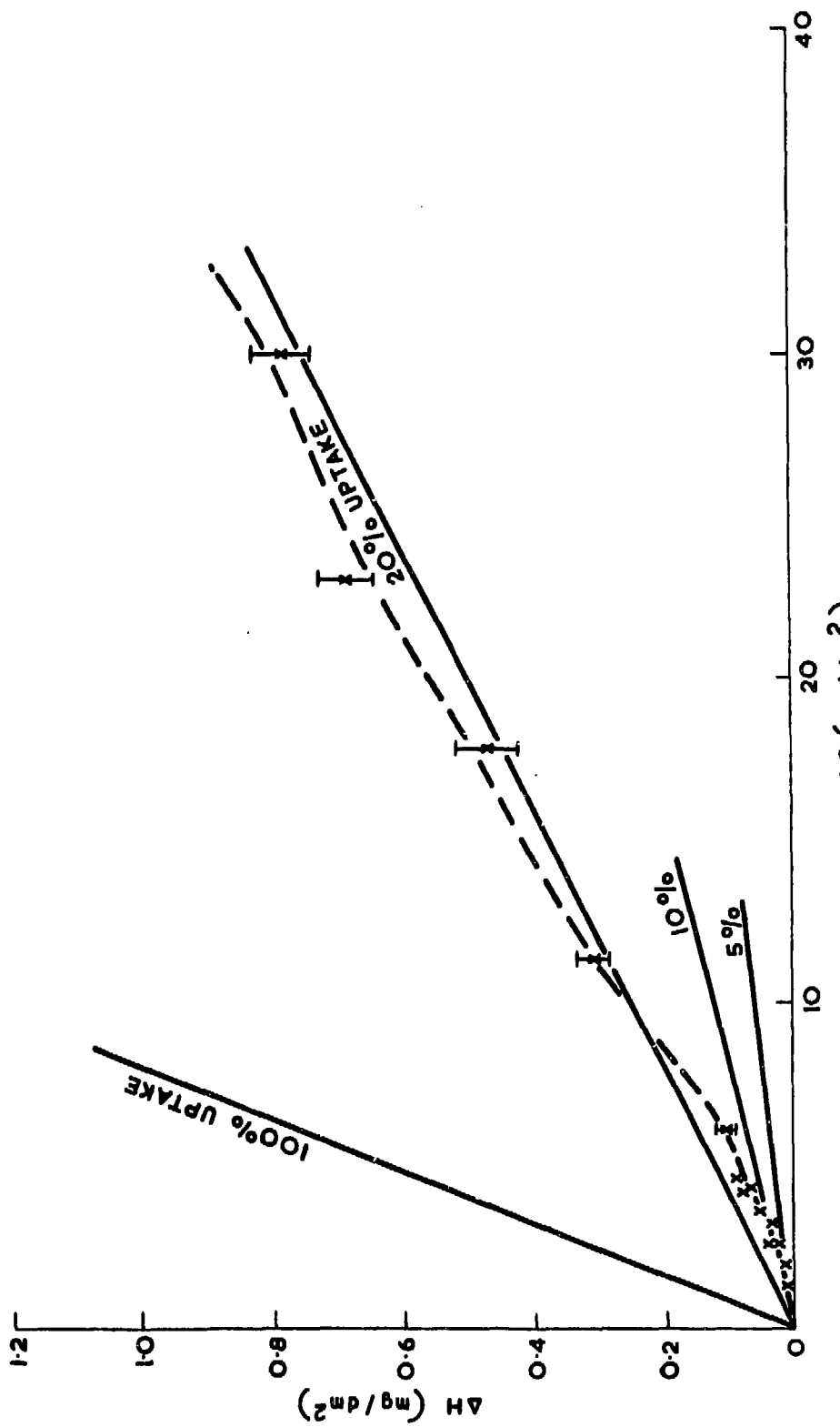

Figure 12: Hydrogen uptake of Zr - 1%Fe in steam at 500°C, 1 atm. (Ref. 20).

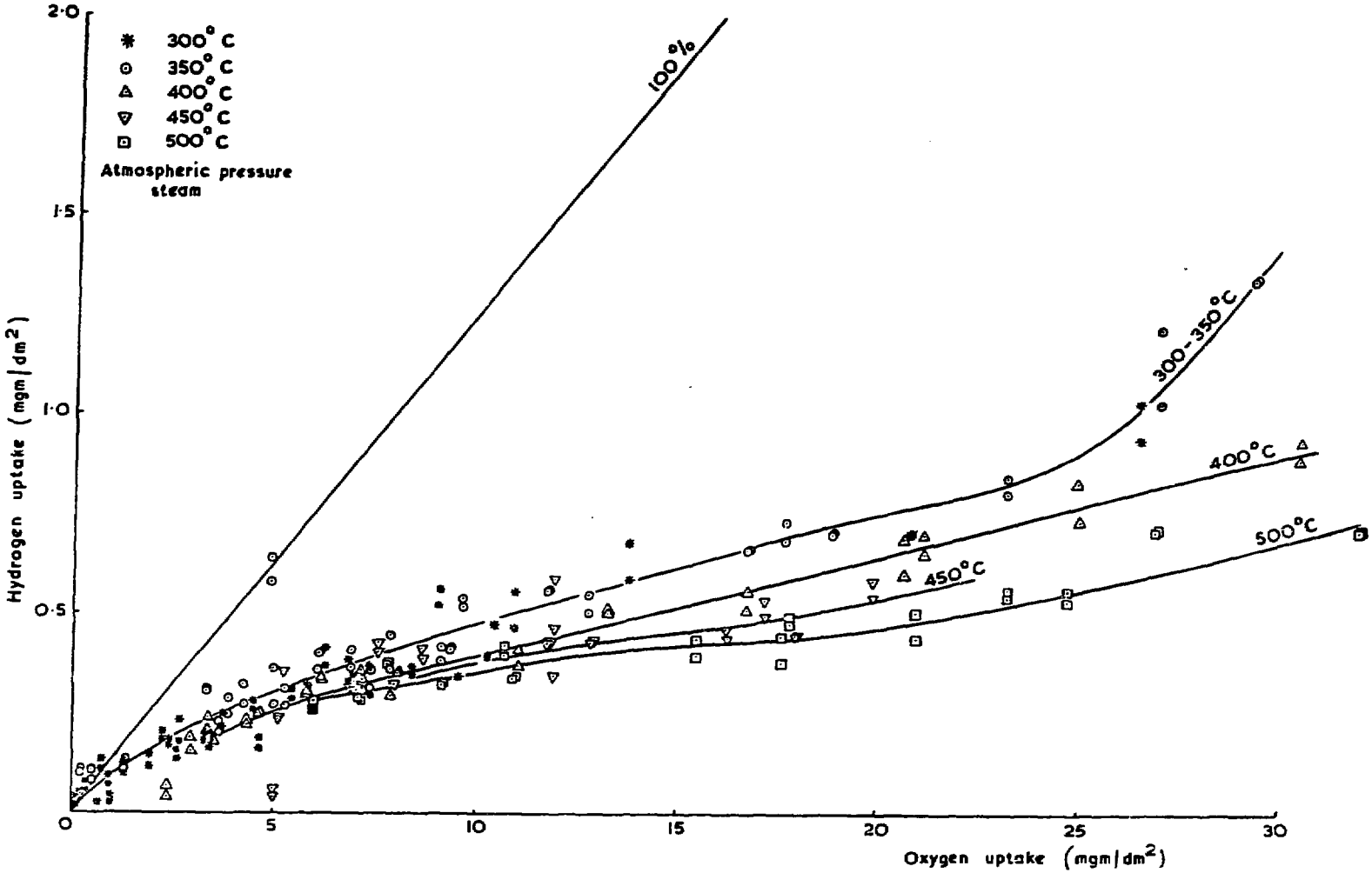

Figure 13: Hydrogen uptake by Zircaloy-2 (I.C.I. 0.005" sheet), from Ref. 15.

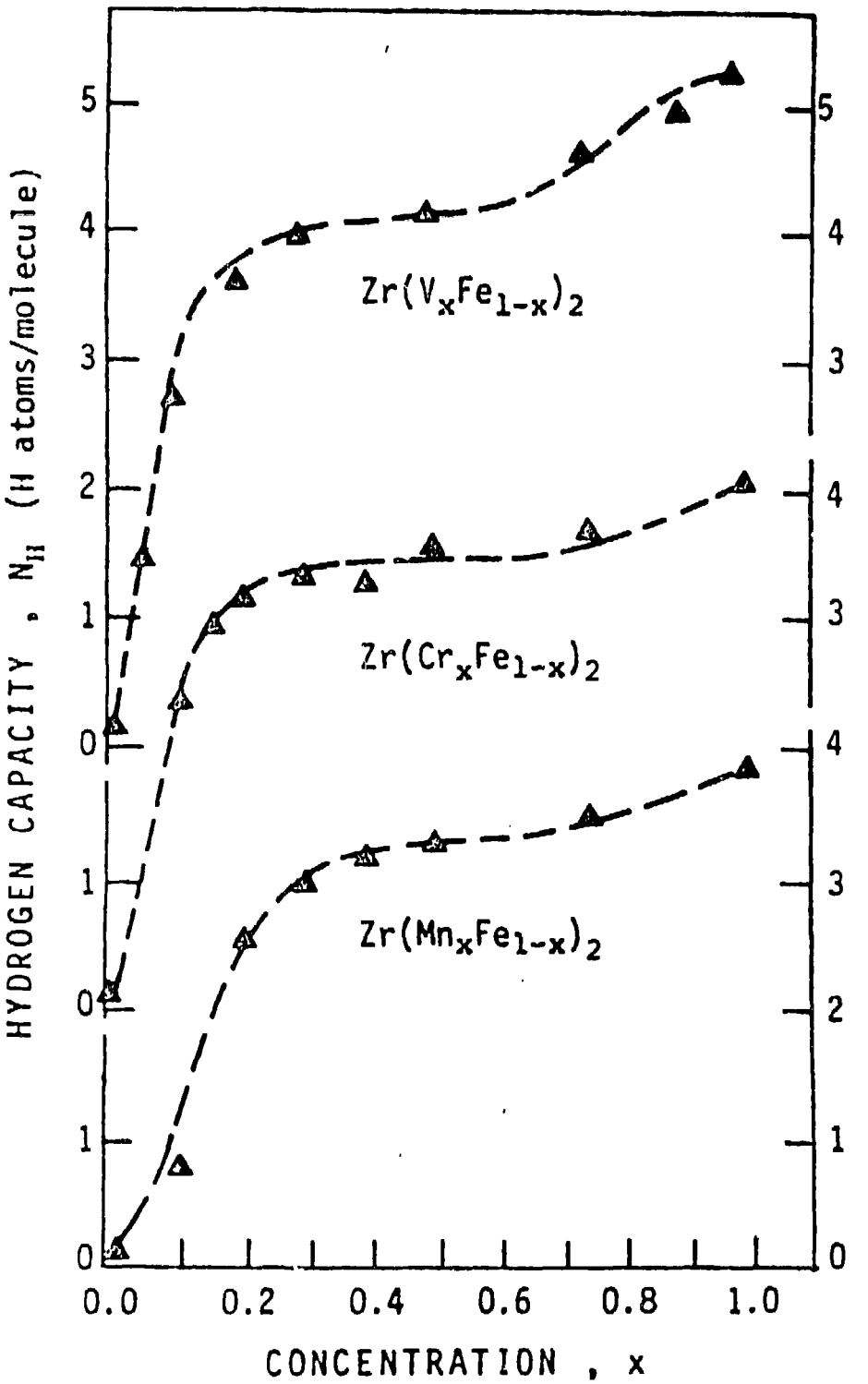

Figure 14: The hydrogen absorption capacity of $Zr(A_xFe_{1-x})_2$ (A = V,Cr,Mn) pseudobinary compounds as a function of the concentration, x. The dashed lines are theoretical fits. (Ref. 29).

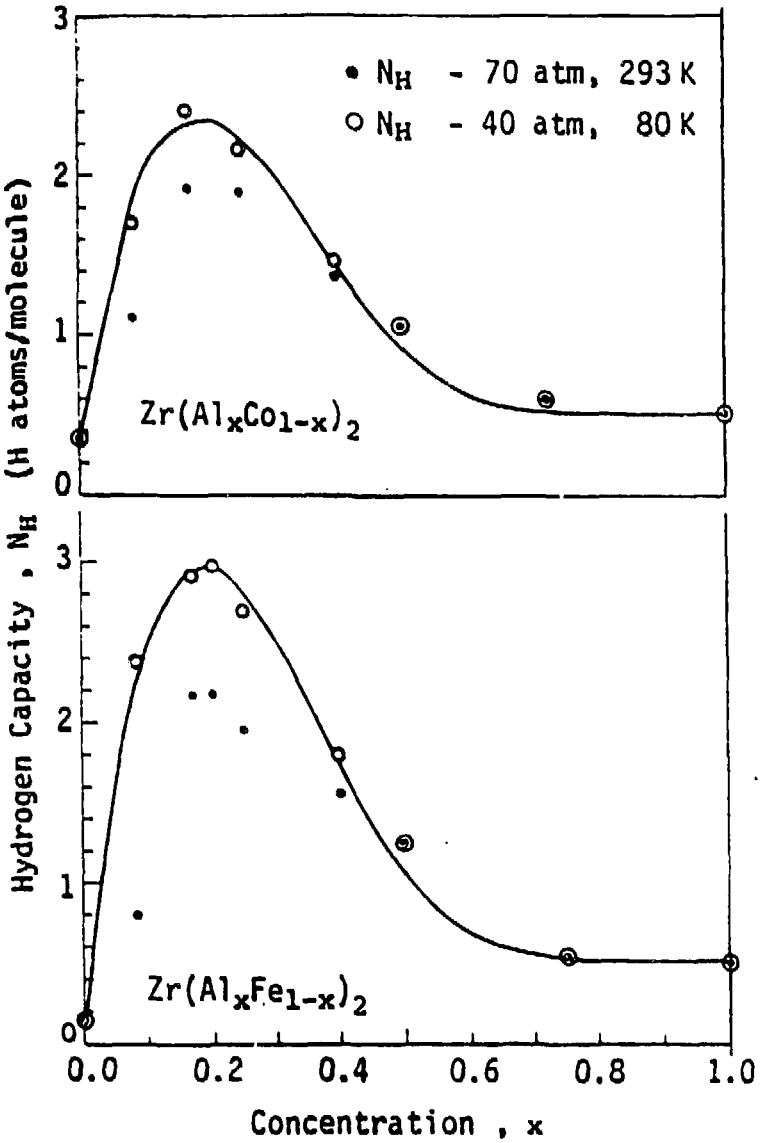

Figure 15: The hydrogen absorption capacity of $Zr(Al_xFe_{1-x})_2$ and $Zr(Al_xCo_{1-x})_2$ as a function of x at room temperature and ~70 atm. (full marks), and at liquid nitrogen temperature and ~40 atm. (open marks). The solid lines are the theoretical results. (Ref. 30).

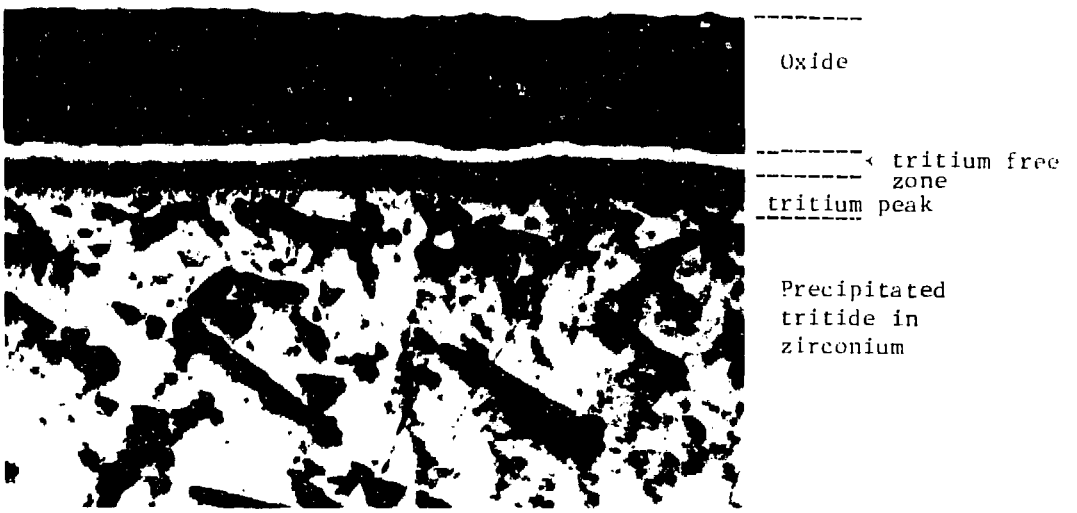

Figure 16: Redistribution of tritium at the oxide-metal interface. (Ref. 63).

Note - Absence of tritium in the metal zone adjacent to the oxide due to the high oxygen level there and, tritium enrichment in the metal zone with low oxygen content.

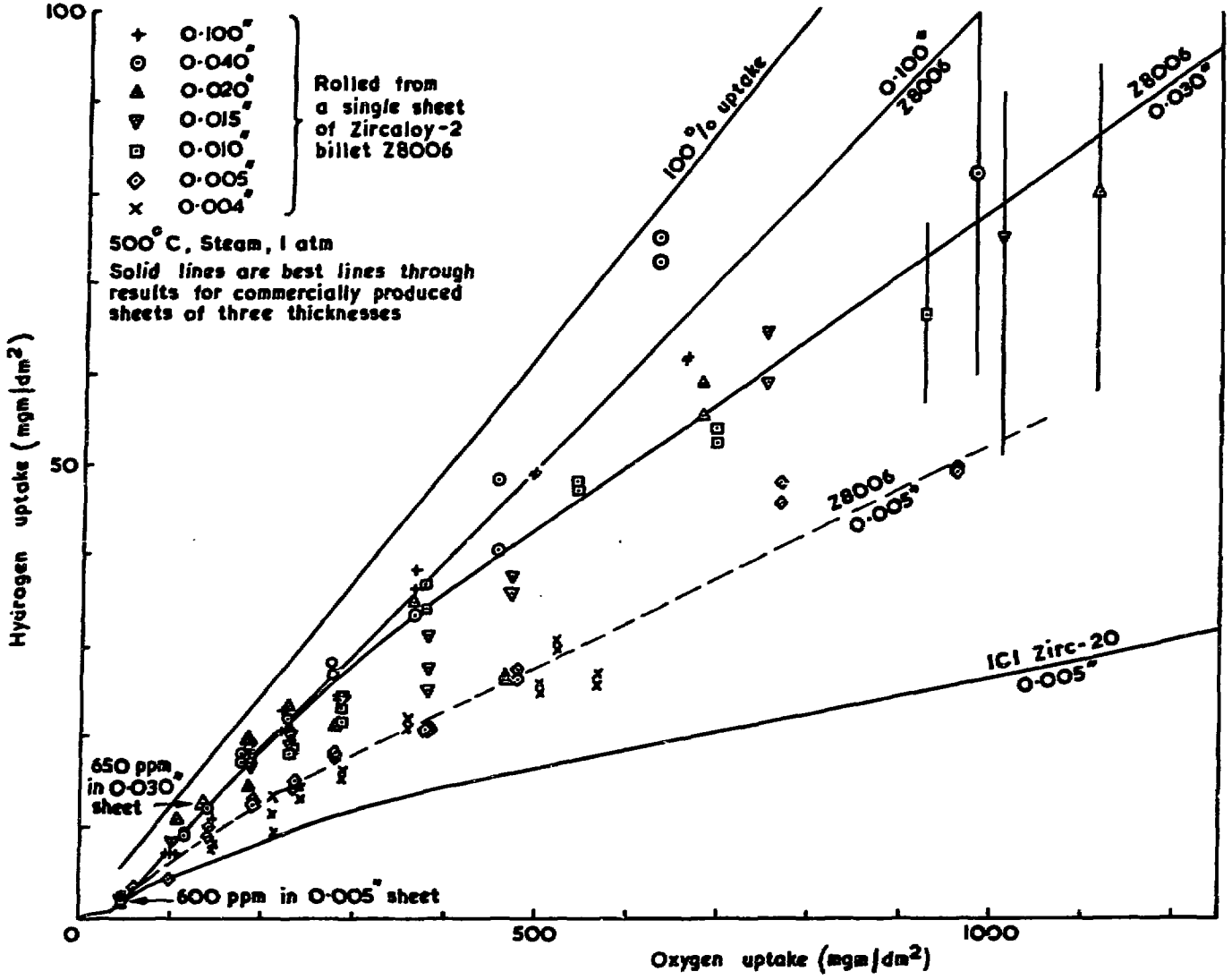

Figure 17: Effect of specimen thickness on hydrogen absorption by Zircaloy-2. (Ref. 15).

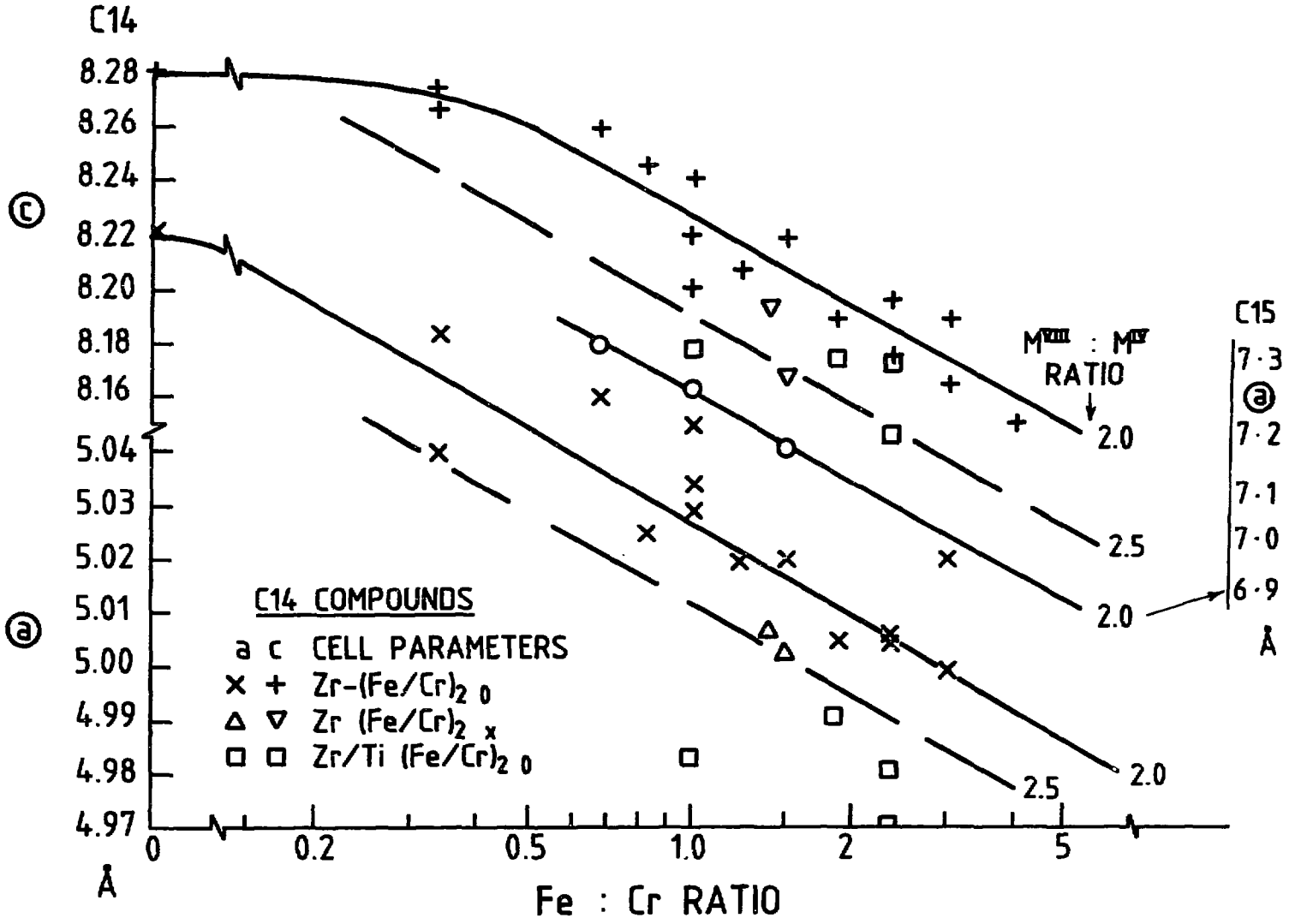

Figure 18: Effect of composition on lattice constants of $Zr(Fe/Cr)_{2+x}$.

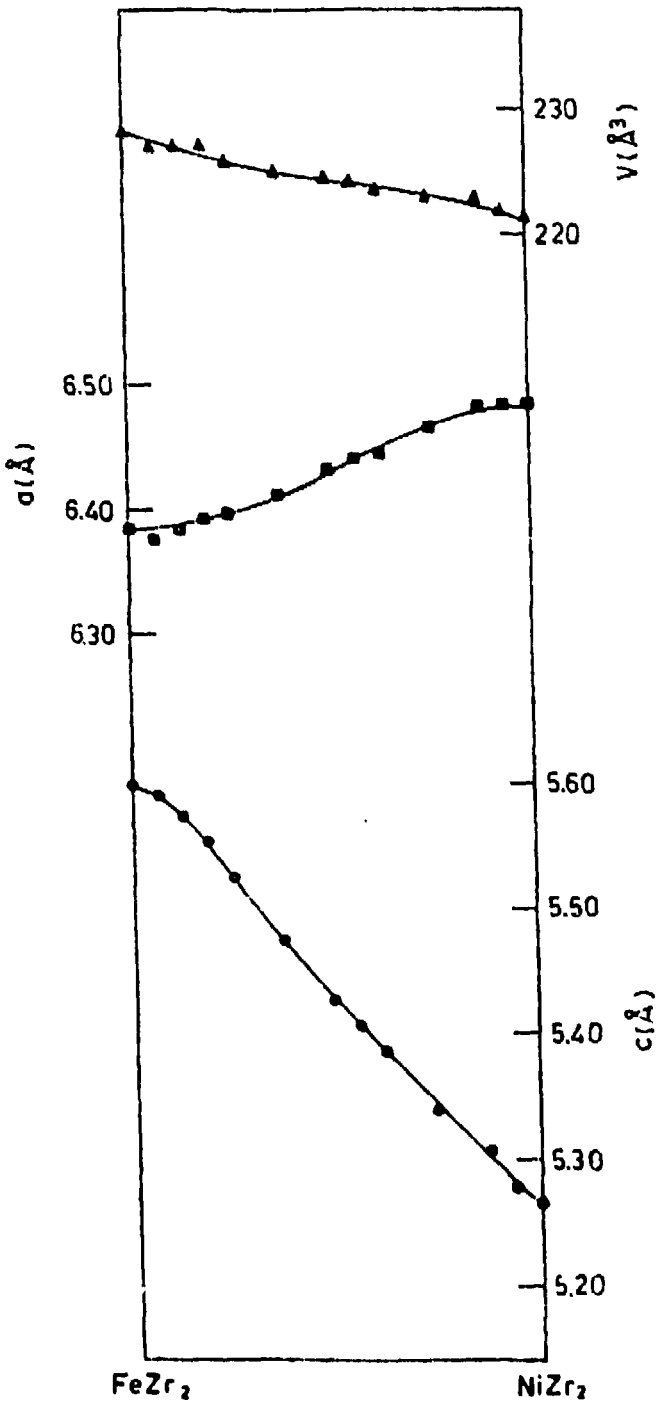

Figure 19: Lattice constants, a and c, and volume, V of the unit cell for the system $Fe_{1-x}Ni_xZr_2$. (Ref. 84).

ISSN 0067 - 0367

To identify individual documents in the series we have assigned an AECL- number to each.

Please refer to the AECL- number when requesting additional copies of this document

from

Scientific Document Distribution Office
Atomic Energy of Canada Limited
Chalk River, Ontario, Canada
K0J 1J0

Price: B

ISSN 0067 - 0367

Pour identifier les rapports individuels faisant partie de cette série nous avons assigné un numéro AECL- à chacun.

Veuillez faire mention du numéro AECL- si vous demandez d'autres exemplaires de ce rapport

au

Service de Distribution des Documents Officiels
L'Energie Atomique du Canada Limitée
Chalk River, Ontario, Canada
K0J 1J0

Prix: B

1130-87